

CHARACTERISTICS OF POLYLACTIDE COMPOSITES
INVOLVING MONTMORILLONITE AND BORON COMPOUNDS

A THESIS SUBMITTED TO
THE GRADUATE SCHOOL OF NATURAL AND APPLIED SCIENCES
OF
MIDDLE EAST TECHNICAL UNIVERSITY

BY

ALİNDA ÖYKÜ AKAR

IN PARTIAL FULFILLMENT OF THE REQUIREMENTS
FOR
THE DEGREE OF MASTER OF SCIENCE
IN
POLYMER SCIENCE AND TECHNOLOGY

FEBRUARY 2016

Approval of the thesis:

**CHARACTERISTICS OF POLYLACTIDE COMPOSITES
INVOLVING MONTMORILLONITE AND BORON
COMPOUNDS**

submitted by **ALİNDA ÖYKÜ AKAR** in partial fulfillment of the requirements
for the degree of **Master of Science in Polymer Science and Technology**
Department, Middle East Technical University by,

Prof. Dr. Gülbin Dural Ünver
Dean, Graduate School of **Natural and Applied Sciences** _____

Prof. Dr. Necati Özkan
Head of Department, **Polymer Science and Technology** _____

Prof. Dr. Jale Hacaloğlu
Supervisor, **Chemistry Dept., METU** _____

Examining Committee Members:

Prof. Dr. Teoman Tinçer
Chemistry Dept., METU _____

Prof. Dr. Jale Hacaloğlu
Chemistry Dept., METU _____

Prof. Dr. Göknur Bayram
Chemical Engineering Dept., METU _____

Prof. Dr. Ceyhan Kayran
Chemistry Dept., METU _____

Prof. Dr. Nursel Dilsiz
Chemical Engineering Dept., Gazi University _____

Date: February 5, 2016



I hereby declare that all information in this document has been obtained and presented in accordance with academic rules and ethical conduct. I also declare that, as required by these rules and conduct, I have fully cited and referenced all material and results that are not original to this work.

Name, Last name: Alinda Öykü AKAR

Signature:

ABSTRACT

CHARACTERISTICS OF POLYLACTIDE COMPOSITES INVOLVING MONTMORILLONITE AND BORON COMPOUNDS

Akar, Alinda Öykü

M.S., Polymer Science and Technology Department

Supervisor : Prof. Dr. Jale Hacaloğlu

February 2016, 93 pages

Poly(lactic acid) (PLA) is a biodegradable and biocompatible polymer and it is accepted as a promising alternative to the petroleum based materials. The main objective of this study is to investigate the effect of the type and the amount of boron compounds with the addition of nanoclay to thermal, mechanical properties and flame retardancy of poly(lactic acid) (PLA) based nanocomposites. By this aim, zinc borate (ZnB), benzene-1,4-diboronic acid (BDBA) and Cloisite 30B (C30B) are used as an additive in PLA matrix.

SEM images of composites indicated homogeneous dispersion of boron compounds in PLA matrix for low concentrations. Agglomerations are observed as the amount of additives is increased. TEM analyses of PLA nanocomposites

indicated intercalated structures. Characteristic Bragg peak of nanoclay disappeared in the XRD diffractograms of nanocomposites in accordance to TEM results.

DSC results pointed out increase in melting temperatures upon incorporation of boron compounds into PLA matrix. TGA analyses revealed that inclusion of boron compounds causes reduction in thermal stability but improvement in char yield of PLA matrix. Generation of cyclic oligomeric products, protonated oligomers and low mass fragments were observed during the pyrolysis of the composites including boron compounds. These reactions, although cause decomposition of PLA chains at low concentrations of boron compounds to a certain extent, generate a cross-linked structure increasing thermal stability at high concentrations of boron compounds. Increase in relative yields of products due to cis-elimination reactions after nanoclay addition was also observed. Incorporation of C30B into PLA composites further increases thermal stability of PLA composites involving BDBA, but, in general, causes a decrease in thermal stability of composites involving ZnB.

Tensile tests indicated that ZnB addition causes increase in tensile strength whereas BDBA addition results in decrease of percent elongation values. No significant difference between flame retardancy of PLA and its composites was detected by UL-94 test. According to LOI test results, addition of boron compounds gives slight improvement on LOI value and the highest LOI value was recorded for ZnB and nanoclay containing composites.

Keywords: Poly(lactic acid) (PLA), Boron Compounds, Zinc Borate (ZnB), Benzene-1,4-Diboronic Acid (BDBA), Montmorillonite, Pyrolysis, Direct Pyrolysis Mass Spectrometry.

ÖZ

MONTMORİLLONİT VE BORON BİLEŞİKLERİ İÇEREN POLİ(LAKTİK ASİT) KOMPOZİTLERİNİN ÖZELLİKLERİ

Akar, Alinda Öykü

Yüksek Lisans, Polimer Bilimi ve Teknolojisi Bölümü

Tez Yöneticisi: Prof. Dr. Jale Hacaloğlu

Şubat 2016, 93 sayfa

Poly(laktik asit) (PLA) biyo-bozunur, biyo-uyumlu bir polimerdir ve zamanla petrol bazlı malzemelere alternatif olacağı öngörülmektedir. Bu çalışmanın amacı; boron bileşiklerinin tipi, miktarı ve nanokil ile birlikte kullanımının PLA bazlı nanokompozitlerin ısısal, mekanik ve yanmayı geciktirme özelliklerine etkisini araştırmaktır. Bu amaç doğrultusunda, PLA matrisine, çinkoborat (ZnB), Benzen-1,4-diboronik asit (BDBA) ve Cloisite 30B (C30B) eklenmiştir.

Kompozitlerin SEM taramaları; bor bileşiklerinin düşük oranlarındaki katkılarının PLA matrisi içinde homojen olarak dağıldığını göstermektedir. Yüksek oranlardaki eklemelerde ise yığılmalar gözlenmektedir. PLA nanokompozitlerin TEM analizinde ise arakatman yapısı görülmektedir. Bu

sonuçlara paralel olarak; nanokompozit yapısında bulunan nanokilin XRD diffraktogramındaki karakteristik Bragg piki ortadan kalkmıştır.

DSC sonuçlarına göre, ham PLA ile kıyaslandığında, borlu bileşik içeren kompozitlerde daha yüksek erime sıcaklığı ve nanokil takviyeli nanokompozitlerde daha yüksek erime piki gözlenmektedir. TGA sonuçları; PLA matrisine borlu bileşiklerin eklenmesinin bozunma sıcaklığında düşmeye, fakat külleşme miktarında artışa sebep olduğunu göstermektedir. Piroliz sırasında, boron bileşikleri içeren PLA'nın trans-esterifikasyon reaksiyonlarına bağlı küçük kütleli fragmantlara ek olarak oligomerik ürünlerin göreceli veriminde artış gözlenmektedir. Bu tip reaksiyonlar, boronun düşük konsantrasyonunda PLA zincirlerinin bozunmasına neden olsa da, borlu bileşiklerin yüksek konsantrasyonlarında çapraz bağlı yapı oluşturarak ısıl kararlılığı artırmaktadır. Bunun yanı sıra, nanokil eklenmesi akabinde cis-eliminasyonu reaksiyonlarından dolayı oluşan ürünlerin göreceli veriminde artış gözlenmektedir. PLA kompozitlerine C30B eklenmesi, BDBA içeren PLA kompozitlerin ısıl kararlılığını daha da artırmakta ama genel olarak ZnB içeren kompozitlerin ısıl kararlılığını azaltmaktadır.

ZnB çekme dayanımında bir miktar artışa, BDBA ise yüzdelik uzamada bir miktar düşüşe neden olmaktadır. UL-94 testi sonuçlarına göre PLA ve kompozitleri arasında yanmayı geciktirme anlamında belirgin bir fark olmadığı görülmüştür. LOI testi sonuçlarına göre, bor bileşiklerinin eklenmesi sonucunda PLA'nın LOI değerinde bir miktar artış gözlemlenmiştir ve en yüksek LOI değeri ZnB ve nanokil içeren kompozitte kaydedilmiştir.

Anahtar kelimeler: Poli(laktik asit) (PLA), Boron Bileşikleri, Çinkoborat (ZnB), Benzen-1,4-diboronik asit (BDBA), Montmorillonit, Piroliz, Direk piroliz kütle spektrometresi.



to my mother...

ACKNOWLEDGEMENTS

I would like to express my sincere appreciation to my supervisor Prof. Dr. Jale Hacalođlu for her endless support, understanding, valuable advices, and encouragement during my works. She contributed me a lot with either her great personality or credible knowledge. During my conversations with her, she helped me to improve my point of view, criticism, determination, and also motivated me with her guidance. She was not just a thesis advisor, but also an admired person and someone taken as an example for me with her trustworthy personality.

I thank Ümit Tayfun for his precious help and contributions for preparation of composite substances. I am greatly indebted to Prof. Dr. Erdal Bayramlı for providing me opportunity of using the instruments in his laboratory.

I would like to thank to Prof. Dr. Teoman Tinçer for giving me the opportunity to study in his laboratory.

I would like to thank to Gencay Çelik for his help in XRD tests of samples and I am greatly indebted to Prof. Dr. Ayşen Yılmaz for providing to use the instrument in her laboratory.

Special thanks to my laboratory mates Müberra Göktaş and Esra Özdemir, and my beloved friends Özlem Güngör, Özge Sıla Gündüz, Mehmet Tefik Özaydın, Süleyman Furkan Yücebaş, Erdem Tekesen, Utku Yağar, Berk Öcalan, Morsaleh Ranjbar Moghaddam, Tuba Kaya Deniz, Kia AF, Talha Güneş who always supported me and I am very lucky to have friends like you.

Last but definitely not the least; I would like to thank to my mother, father and my little sister ADA for loving me and their endless support, encouragement and patience during this study.



TABLE OF CONTENTS

ABSTRACT	v
ÖZ.....	vii
ACKNOWLEDGEMENTS	x
TABLE OF CONTENTS	xii
LIST OF FIGURES	xvi
LIST OF SCHEMES	xix
LIST OF ABBREVIATIONS	xx
CHAPTERS.....	1
1. INTRODUCTION.....	1
1.1. Biodegradability of Polymers	3
1.1.1. Biodegradable Polymers Derived from Petroleum Resources	4
1.1.2. Biodegradable Polymers Derived from Natural Resources.....	4
1.2. Poly(lactic acid), (PLA)	5
1.2.1. PLA Production and Applications.....	6
1.2.2. PLA Advantages	8
1.2.3. PLA Limitations and Adverse Effects	9
1.3. Degradation Mechanism of PLA	10
1.3.1. Photolysis	10
1.3.2. Hydrolytic Degradation.....	10
1.3.3. Alkali-Catalyzed Hydrolysis	11

1.3.4. Acid-Catalyzed Hydrolysis	11
1.3.5. Thermal Degradation Mechanisms of PLA	11
1.4. Commercialization of PLA	12
1.4.1. Additives Used for Enhancement of PLA matrix	13
1.5. Improvement of Thermal Degradation and Flame Retardant Characteristics of PLA	14
1.5.1. Thermal Stability of Polymers	14
1.5.2. Heat Stabilizers	15
1.5.3. Flame Retardants	15
1.6. Reinforcement of PLA	19
1.6.1. Improvement of Properties of PLA via Montmorillonite (MMT) ..	21
1.7. Preparation of PLA Nanocomposites	23
1.8. Boron Compounds and Nanoclay Containing PLA Composites	24
1.9. Objective of This Thesis	26
2. EXPERIMENTAL	27
2.1. Materials Used for Preparation of Nanocomposites	27
2.2. Preparation of Nanocomposites	28
2.2.1. Melt Blending Method	28
2.3. Apparatus Used for Characterization Techniques	31
2.3.1. Structural & Morphological Analysis	31
2.3.2. Thermal Analysis	32
2.3.4. Mechanical Analysis	33
3. RESULTS AND DISCUSSION	35
3.1. Morphological Analysis	35

3.1.1.	Scanning Electron Microscope (SEM)	35
3.1.2.	Transmission Electron Microscope (TEM)	38
3.1.3.	X-Ray Diffractometer (XRD).....	40
3.2.	Thermal Analyses	43
3.2.1.	Differential Scanning Calorimetry (DSC) Analyses	43
3.2.2.	Thermogravimetric (TGA) Analyses.....	47
3.2.3.	Direct Pyrolysis Mass Spectrometry (DP-MS) Analyses.....	50
3.3.	Mechanical Properties.....	67
3.3.1.	Tensile Test	67
3.4.	Flammability Properties.....	73
3.4.1.	UL-94 Ratings	73
3.4.2.	LOI Ratings	74
4.	CONCLUSIONS.....	77
	REFERENCES	81

LIST OF TABLES

TABLES

Table 1.1. Examples of polymer additives [30].	13
Table 1.2. Common ZnB formulations [37].	18
Table 2.1. Specifications of organically modified Cloisite 30B.	27
Table 2.2. Specifications of boron compounds.	28
Table 2.3. Composition of PLA nanocomposites prepared by melt blending technique.	29
Table 3.1. DSC test results of neat PLA, PLA involving variable amounts of boron compounds and PLA-boron composites containing 3% wt. nanoclay... 46	
Table 3.2. TGA data for PLA, PLA/boron compounds with or without 3% C30B.	48
Table 3.3. Tensile strength, percentage strain and Young's modulus properties for PLA, PLA with boron additives and PLA/boron compounds/organoclay composites.	68
Table 3.4. UL-94 ratings and observations during UL-94 test for the samples prepared.	73
Table 3.4. (Continued) UL-94 ratings and observations during UL-94 test for the samples prepared.	74

LIST OF FIGURES

FIGURES

Figure 1.1. Schematic view of the migration of the layered silicates during burning [39].	19
Figure 3.1. SEM images of ZnB and PLA-ZnB composites with 1%, 2% and 3% concentrations of ZnB at x500 magnification.	36
Figure 3.2. SEM images of BDBA and PLA-BDBA composites with 1%, 2% and 3% concentrations of BDBA at x500 magnification.	37
Figure 3.3. TEM images of 3% nano clay containing PLA-ZnB and PLA-BDBA composites at low (x1000) and high (x10,000) magnifications.	39
Figure 3.4. XRD patterns of neat PLA, ZnB and PLA-ZnB composites at different concentrations.	40
Figure 3.5. XRD patterns of neat PLA, BDBA and PLA-BDBA composites at different concentrations.	41
Figure 3.6. XRD patterns of neat PLA, nanoclay and PLA-ZnB-NC composites.	42
Figure 3.7. XRD patterns of neat PLA, nanoclay and PLA-BDBA-NC composites.	43
Figure 3.8. DSC thermograms of neat PLA, PLA involving variable amounts of ZnB (1, 2, 3 wt. %) and PLA-ZnB composites containing 3% wt. Cloisite 30B.	44
Figure 3.9. DSC thermograms of neat PLA, PLA involving variable amounts of BDBA (1, 2, 3 wt. %) and PLA-BDBA composites containing 3% wt. Cloisite 30B.	45

Figure 3.10. TGA curves of PLA composites containing boron compounds with different compositions and PLA-boron composites with nanoclay addition. ...	49
Figure 3.11. a) The TIC curve, b) the pyrolysis mass spectrum and c) the single ion evolution profiles of fragments recorded during the pyrolysis of PLA.	51
Figure 3.12. Pyrolysis mass spectrum of NC.	53
Figure 3.13. a) The TIC curve, b) the pyrolysis mass spectrum and c) the single ion evolution profiles of selected fragment recorded during the pyrolysis of BDBA.	54
Figure 3.14. The TIC curves and the pyrolysis mass spectra of PLA and PLA composites involving 1, 2, and 3 % ZnB.	55
Figure 3.15. The single ion evolution profiles of selected fragment recorded during the pyrolysis of PLA and PLA composites involving 1, 2, and 3 % ZnB.	56
Figure 3.16. The TIC curves and the pyrolysis mass spectra of PLA-NC and PLA-NC composites involving 1, 2, and 3 % ZnB.	58
Figure 3.17. The single ion evolution profiles of selected fragment recorded during the pyrolysis of PLA-NC and PLA-NC composites involving 1, 2, and 3 % ZnB.	59
Figure 3.18. The TIC curves and the pyrolysis mass spectra of PLA and PLA composites involving 1, 2, and 3% BDBA.	62
Figure 3.19. The single ion evolution profiles of selected fragment recorded during the pyrolysis of PLA and PLA composites involving 1, 2, and 3 % BDBA.	63
Figure 3.20. The TIC curves and the pyrolysis mass spectra of PLA-NC and PLA-NC composites involving 1, 2, and 3% BDBA.	65
Figure 3.21. The single ion evolution profiles of selected fragment recorded during the pyrolysis of PLA-NC and PLA-NC composites involving 1, 2, and 3 % BDBA.	66

Figure 3.22. Tensile strengths of PLA, PLA with boron additives and PLA-boron compounds-organoclay nanocomposites..... 70

Figure 3.23. Percentage elongation of PLA, PLA with boron additives and PLA/boron compounds/organoclay nanocomposites. 71

Figure 3.24. Young's modulus of neat PLA, PLA with boron additives and PLA/boron compounds/organoclay nanocomposites. 72

Figure 3.25. The LOI values of composites. 75



LIST OF SCHEMES

SCHEMES

Scheme 1.1. Lactic acid optical monomers [23].	6
Scheme 1.2. Reaction schemes to produce PLA [23].	7
Scheme 3.1. Thermal degradation of poly(lactic acid).	51
Scheme 3.2. (Continued) Thermal degradation of poly(lactic acid).	52
Scheme 3.3. Degradation of polylactide by hydrolysis reaction.	57
Scheme 3.4. Trans-esterification reactions between the organic modifier of Cloisite 30B and PLA.....	60
Scheme 3.5. Reaction between OH groups of BDBA with ester groups of PLA.	64

LIST OF ABBREVIATIONS

BDBA	Benzene-1,4-diboronic acid
C30B	Cloisite 30B
DP-MS	Direct Pyrolysis Mass Spectrometer
NC	Nanocomposite
PCL	Poly(caprolactone)
PET	Poly(ethylene terephthalate)
PHA	Poly(hydroxyalkanoate)
PHB	Poly(hydroxybutyrate)
PLA	Poly(lactic acid)
PS	Polystyrene
PVA	Poly(vinyl alcohol)
PVC	Poly(vinyl chloride)
T_c	Crystallization temperature
T_g	Glass transition temperature
TIC	Total ion current
T_m	Melting temperature
ZnB	Zinc borate



CHAPTER 1

INTRODUCTION

The word polymer is derived from the classical Greek words poly meaning “many” and meros meaning “parts.” Simply stated, a polymer is a long-chain molecule that is composed of a large number of repeating units of identical structure [1, 2]. The polymerization is a chemical reaction in which two or more substances combine together to form a molecule of higher molecular weight. The product is called polymer and the starting material is called monomer [2, 3].

Polymers are being used by humans since antiquity. Biopolymers were derived from natural resources before the advent of industrial revolution. For example, natural rubber was discovered and used by Mesoamericans sometime before 1600 B.C. Early synthetic polymers such as nitrocellulose was produced using plant derived cellulose and nitric acid (in 1862). First truly synthetic polymer, Bakelite, was synthesized by using phenol and formaldehyde in year 1907 [4].

During the exploitation of the petroleum resources for fueling the industry; petroleum based polymers were also developed with this new and seemingly abundant source; fossil fuel. Also, the advances in chemistry and chemical industry opened new opportunities for synthesizing new materials and imitation of scant natural materials. Before and during World War II, due to scarcity of natural rubber; new processes were developed to produce synthetic rubber. First successful product as a substitute was made possible by BASF in the 1930s with production of synthetic polystyrene. Nylon, polyethylene and poly(vinyl chloride) (PVC) were among the first commercially produced synthetic polymers and these materials have led to new commercial products and

applications. For example, discovery of poly(ethylene terephthalate), PET, led the phasing out of glass in packaging/bottling of the liquids which resulted in cheaper products and more widespread usage [4].

Industry has flourished by the advance of petro-chemistry and polymer technologies which has been rewarding and useful for the society [5]. Textiles, paints, structural materials, insulation materials, rubbers, dyes, adhesives, device cases, packaging, tires, etc. are common uses for polymers [6, 7].

The vast number of different polymers might be confusing and tiresome. Conveniently, polymers can be classified in many different ways by their characteristics. These groups are useful for general identification of various properties of polymers [7]. The most important classification is based on the origin of the polymer, i.e., natural vs. synthetic. Other classifications are based on the polymer structure, polymerization mechanism, preparative techniques, or thermal behavior [8]. In addition, the biodegradability of the polymeric material plays very important role for characterization due to recent environmental concerns. Biodegradable polymers may be considered as safe for the environment [9, 10], and are an interesting alternative to conventional polymers [5, 7, 11]. Production of petrochemical-based polymers rely on fossil fuels and eventually ends up as non-degradable waste. These wastes are significantly disturbing and damaging the environment. Incineration of these wastes produces large amounts of carbon dioxide which causes global warming [9]. So, a more environment friendly approach of polymer production was needed to minimize this impact. Bio-degradable polymers are the result of this quest. The biodegradability of these green polymers is much better when compared to their petro-chemical counterparts which linger in nature for centuries without any visible sign of degradation. But, their performance is as not good as conventional polymers, so properties of bio-degradable polymers needs to be improved for better faring in industrial uses [6].

1.1. Biodegradability of Polymers

Biodegradable polymers were first introduced in 1980s due to arising environmental concerns. There are many sources of biodegradable plastics, either synthetic or natural polymers. Natural polymers are available from renewable sources, while synthetic polymers are produced from non-renewable resources (fossil fuels) [12].

Biodegradable polymers are degraded by the action of biological agents (e.g., microorganisms, bacteria or fungi) in nature over relatively short time period with respect to petroleum based polymers. For a material to be considered as biodegradable, it is necessary to set a time frame for degradability, defining the environmental conditions under which degradation is supposed to occur (temperature, pH and moisture) and also to what extent the polymer should degrade [11-13]. Biodegradability depends not only on the origin of the polymer but also on its chemical structure [12]. Most of the commodity polymers, polyethylenes, poly(ethylene terephthalate), (PET), poly(vinyl chloride), (PVC), polystyrene, (PS), polyurethane, (PU) etc are not biodegradable [11].

“In the case of traditional petroleum-derived plastics, their durability which make them ideal for many areas of applications, such as packaging, building materials, commodities and hygiene products, can lead to waste-disposal problems, as these materials are not readily biodegradable [13]. Because of their resistance to microbial degradation, they accumulate in the environment and cause pollution. Additionally, in recent times oil prices have increased markedly. These facts have helped to stimulate interest in biodegradable polymers and in particular biodegradable biopolymers” [10, 12].

Although, the development and commercialization of biodegradable polymers is relatively recent (since 2000s), a rapid growth of this industry is anticipated due to environmental concerns. Some of these biodegradable polymers are

poly(lactic acid) (PLA), poly(hydroxyalkanoates) (PHA), and poly(caprolactones) [11].

Main reason that prevents widespread usage of biodegradable polymers is their relatively short durability. So, if this problem could somehow be eliminated, the usage of these polymers could be spread. The most convenient method being used for increasing durability is the incorporation of additive materials into the polymer chain/matrix. Eventually, the mechanical behavior of biodegradable materials depends on their chemical composition and processing characteristics which affect their area of usage [12].

Biodegradable polymers could be produced by using several raw materials of different origins. These resources are divided in two general classes; petroleum resources (non-renewable resources) and biological resources (renewable resources) [5].

1.1.1. Biodegradable Polymers Derived from Petroleum Resources

These are synthetic polymers with hydrolysable functions, such as ester, amide and urethane, or polymers with carbon backbones, in which additives like antioxidants are added. Recent developments in this area have resulted in commercial grade petroleum-based biodegradable polymers [2, 5, 12]. However, the applications of these materials are rare and not sufficient for industrial usage except niche usage (medicine [12], prosthesis [14], etc.).

1.1.2. Biodegradable Polymers Derived from Natural Resources

Enzymes, nucleic acids and proteins are polymers of biological origin. Starch, cellulose and natural rubber are examples of polymers of plant origin and polymers such as enzymes and proteins could be found in both animals and

plants as constituents. There are a large number of synthetic polymers consisting of various families: fibers, elastomers, plastics, adhesives, etc. [7, 8, 15].

Most of the biodegradable polymers are obtained from natural precursors such as cellulose, acetate, lactic acid, etc. The polymers obtained from these precursors are generally biodegradable (exceptions might occur). Some examples of these biodegradable polymers are polyethers, polyesters, polycaprolactones, polylactides, polyurethane, poly(vinyl alcohol) and polyamide, etc. [2, 5].

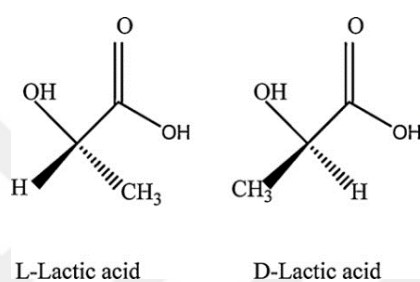
Amongst these polymers, poly(lactic acid) (PLA) is a good choice of biodegradable material due to its excellent properties such as melting point and superior mechanical properties [16]. Degradation mechanism of PLA depends on molecular weight, temperature, pH, impurities, and active groups in molecule structure and in reaction medium [17].

1.2. Poly(lactic acid), (PLA)

“Poly(lactic acid), (PLA) is a compostable polymer which is derived from renewable sources (e.g. starch and sugar). Until recently, the main usage area of PLA has been limited to medical applications such as implant devices, tissue scaffolds, and internal sutures; mostly due to its high cost, low availability and limited molecular weight [2, 5]. Discovery of the new techniques, which allow economical production of high molecular weight PLA polymer have widened its usage [18]. Since PLA is compostable and derived from renewable sources, it has been viewed as a savior material to reduce the municipal solid waste disposal problem. Its low toxicity and environmentally benign characteristics [2, 10, 18, 19] has made PLA an ideal material for food packaging and for other consumer products” [13, 20, 21].

1.2.1. PLA Production and Applications

PLA is a linear, aliphatic polyester synthesized from lactic acid monomers by condensation polymerization of lactic acid, or by catalytic ring-opening polymerization of the lactide (dilactone of lactic acid) [5, 10, 13, 21, 22]. These precursors are derived from the fermentation of organic materials produced by agricultural industries. Lactic acid exists as two optical isomers, L- and D-lactic acid, which are shown in Scheme 1.1. Commercially available PLA grades are copolymers of poly (L-lactide) with meso-lactide or D-lactide [5, 21-24].

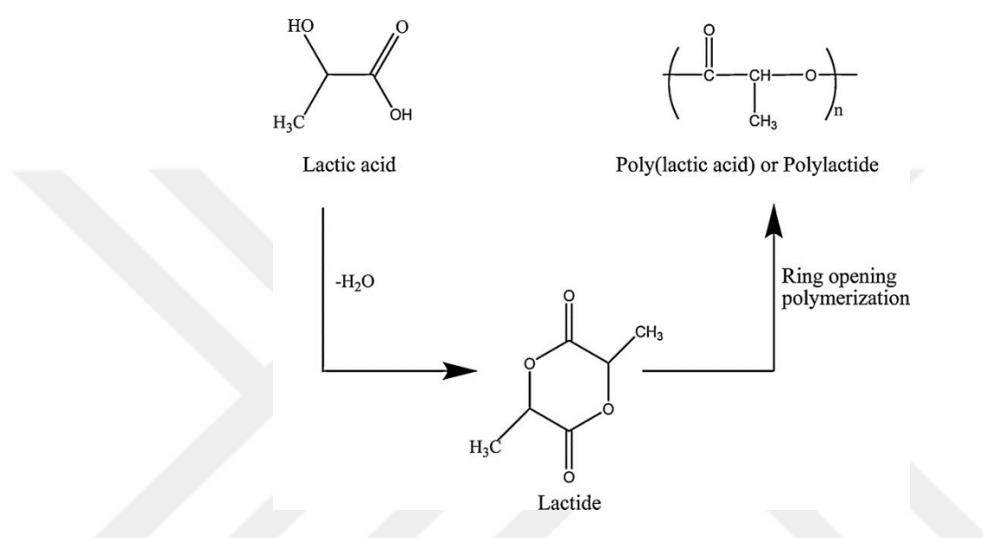


Scheme 1.1. Lactic acid optical monomers [23].

PLA has acceptable mechanical properties, thermal plasticity, and biocompatibility, thus, a promising polymer for various applications [2]. The amount of D-enantiomers is known to affect the properties of PLA, such as melting temperature, degree of crystallinity and mechanical properties [25]. So, varying concentrations of D and L enantiomer mixtures are used for copolymerization of polymers with different properties [22, 24].

The L-lactic acid twists a passing polarized light source clockwise, and D-lactic acid twists counter clockwise. Lactic acid derived from petrochemical resources is an optically inactive 50/50 mixture of the d and l forms. Since the fermentation approach uses renewable resources, its usage became prevalent since the 1990s [10, 18, 22, 23].

Polymerization of lactic acid to PLA is conducted by a direct condensation process using solvents under high vacuum. As an alternative to this process, a cyclic dimer intermediate called lactide is formed, and then via catalytic ring-opening polymerization of the cyclic lactide without using solvents, PLA is produced [23]. These schemes are shown in Scheme 1.2.



Scheme 1.2. Reaction schemes to produce PLA [23].

Low molecular weight PLA usually has substandard mechanical properties [22]. In addition, solvent removal and the effect of solvent on polymer under high vacuum and temperature affect the structural and mechanical properties of the polymer. Hence, these techniques cause racemization of PLA and discoloration. Because of these disadvantages of direct polycondensation, the commercial manufacture of PLA utilizes lactide ring opening polymerization [23].

1.2.2. PLA Advantages

PLA has important advantages, such as being eco-friendly, biocompatible and thermally processable compared to other biopolymers.

- a) Eco-friendly: PLA is biodegradable, recyclable, and compostable as being derived from renewable and sustainable resources (e.g., corn, wheat, or rice). Its production also captures carbon dioxide. As a result of sustainability and eco-friendly characteristics, PLA is an attractive biopolymer [5, 10, 18, 22, 23, 26].
- b) Biocompatibility: The most tempting aspect of PLA; especially with respect to biomedical applications; is its biocompatibility. A biocompatible material, by definition, should not produce toxic or carcinogenic effects in local tissues and the degradation products should not interfere with tissue healing. PLA hydrolyzes to its constituent hydroxyl acid when implanted in living organisms like the interior of the human body. After hydrolysis, the resultant metabolites are incorporated into the tricarboxylic acid cycle and excreted from the body [5, 10, 22, 23]. PLA degrades usually by hydrolysis and rarely by microbial attack. At higher temperatures and humidity, high molecular weight PLA is not contaminated by microbes [22].
- c) Processibility: PLA has better thermal processibility when compared to other biopolymers such as poly(hydroxyl alkanates), (PHAs), poly(ethylene glycol) (PEG), poly(caprolactone) (PCL), etc. PLA can be processed by widely used industrial processes like injection molding, film extrusion, blow molding, thermoforming, fiber spinning, and film forming, etc. [5, 23].

1.2.3. PLA Limitations and Adverse Effects

Beyond its advantages, PLA has also some limitations and adverse effects, which are detailed below.

- a) Poor toughness: PLA is a rather brittle material with less than 10% elongation at break. Although its tensile strength and elastic modulus are at par with poly(ethylene terephthalate) (PET), the lower toughness of PLA limits its use to applications that need plastic deformation at higher stress levels [23].
- b) Slow degradation rate: PLA degrades by the hydrolysis of backbone ester groups [22] and rate of degradation depends on factors like the crystallinity, molecular weight, molecular weight distribution, morphology, water diffusion rate and stereoisomeric content of the polymer. The degradation rate is often considered as the decisive criterion for biomedical applications. The slow degradation rate also poses a problem with the disposal of consumer commodities as well [23].
- c) Hydrophobicity: PLA is relatively hydrophobic with a static water contact angle of approximately 80°. This results in low cell affinity and might trigger an inflammatory response from the surrounding tissue with direct contact.
- d) Lack of reactive side-chain groups: PLA is a chemically inert polymer that has no reactive side-chain groups, which complicates its surface and bulk modification [23].
- e) Harmful effect: In nature, it forms lactide which is an antibacterial agent. Lactide therefore is harmful for environment.

1.3. Degradation Mechanism of PLA

Polymer degradation takes place through scission of the main chains or side-chains of macromolecules, induced by photolysis, hydrolysis, thermal activation, oxidation, or radiolysis [5].

1.3.1. Photolysis

Photolysis with UV light and gamma irradiation of polymers generate radicals and/or ions that often lead to cleavage and crosslinking. Oxidation also occurs concurrently, which complicates the situation, since exposure to light is seldom in the absence of oxygen. Generally this condition changes the material's susceptibility to biodegradation. It is expected that the observed rate of degradation should increase until most of the fragmented polymer is consumed and a slower rate of degradation should follow afterwards for the crosslinked portion of the polymer [10].

1.3.2. Hydrolytic Degradation

“Hydrolytic degradation is the scission of chemical bonds in the polymer backbone by consuming water to form oligomers and ultimately monomers. First, the water molecules attack the water-labile bonds by either directly on the polymer surface or by soaking into the polymer matrix which is followed by bond hydrolysis. In addition to nucleophilic attack by H₂O (neutral hydrolysis), the hydrolysis could also be accelerated with an acid, base or enzyme” [5].

1.3.3. Alkali-Catalyzed Hydrolysis

“Degradation of the polymer under alkaline conditions starts with the attack of the hydroxide anion at the carbonyl carbon of the ester group, thus, generating a tetrahedral intermediate. This step is reversible and the hydroxyl attached to the tetrahedral intermediate can separate, thus the regeneration of the ester occurs. However, the ether connected to the tetrahedral intermediate (RO-) can leave instead, resulting in hydrolysis, causing the generation of an alcohol and carboxylic acid. The preference of the tetrahedral intermediate toward hydrolysis instead of ester regeneration is determined by the ability of the leaving alcohol (R-OH) to stabilize a negative charge; therefore, esters formed from acidic alcohols hydrolyze much faster compared to the ester formed from aliphatic alcohols. Ultimately, one hydroxyl and one carboxyl end group are produced as the final product” [5].

1.3.4. Acid-Catalyzed Hydrolysis

At low pH conditions; degradation of polyesters begins with the protonation of the carbonyl oxygen of the ester group with a hydronium ion, which in turn makes the carbonyl carbon more electrophilic due to the positive charge. Afterwards, the attack of water molecules on the carbonyl carbon, also generates a tetrahedral intermediate similar to the one generated during base-catalyzed hydrolysis. The tetrahedral intermediate may either decompose into carboxylic acid and alcohol, or regenerate back to the original ester. Ultimately, protonation of the chain oxygen atom of the ester group and the reaction with water afterwards produces one hydroxyl and one carboxyl end group [5].

1.3.5. Thermal Degradation Mechanisms of PLA

The thermal degradation of PLA usually happens during thermal processing of the material causing a rapid reduction of molecular weight which in turn affects

the final properties of the material, such as the mechanical strength. Thermal degradation of PLA originates from a random main-chain scission reaction, and also depolymerization by back-biting (intramolecular trans-esterification), oxidative degradation, and inter-chain trans-esterification reactions. Moreover; the reactive end groups, residual catalyst, unreacted starting monomer and other impurities contribute to the thermal degradation of PLA. Majority of the efforts in studies regarding PLA research are aimed at the suppression of the polymer degradation in the melt [27-29].

Considering trans-esterification reactions, there exist two types: intramolecular and intermolecular. Intramolecular trans-esterification, or "back-biting", leads to polymer degradation and the formation of cyclic polylactide oligomers. On the other hand, intermolecular trans-esterification affects the sequence of different polymeric segments. As a result, such reactions adversely affect the molecular weight, and henceforth the mechanical properties of the material decreases [29].

The pyrolytic elimination, generating molecules with acrylic end-groups, is a less important side reaction. However degradation processes through radical reactions need to be taken into consideration only for temperatures exceeding 250 °C. On the other hand, hydrolytic degradation reactions can also take place as a competitive reaction depending on the water content [27].

1.4. Commercialization of PLA

PLA has gained enormous attention in industry, due to its biodegradable and biocompatible properties. However, unitary structure and poor properties of PLA such as the inherent brittleness, poor melt strength, low heat deflection temperature (HDT), narrow processing window and low thermal stability poses considerable scientific challenges and limits the applications of PLA. So, it is needed to enhance the versatility of PLA bioplastics, so that they can compete

with conventional polymers. One way to comply with the needs of the industry is to use additives for enhancement of PLA properties [30].

Also, some properties of PLA could be enhanced further by the incorporation of nanoparticles into the polymer matrix; hence forming “nanocomposites”. These nanocomposites are already a part of many large-scale worldwide businesses: automotive (molded parts in cars), electronics and electrical engineering, household products, packaging industry, aircraft interiors, appliance components and security equipment [31].

1.4.1. Additives Used for Enhancement of PLA matrix

Several types of additives could be utilized to improve the characteristics of PLA. These well-established additives included antioxidants, heat stabilizers, light stabilizers, impact modifiers and several others addressing the requirements of modification for standard plastics and today's mass applications [30].

Some examples of groups of additives are given in Table 1.1, below.

Table 1.1. Examples of polymer additives [30].

Plasticizers	Glycerol, Triethyl-Tributyl-Acetyltriethyl-Acetyltributyl Citrate, Poly(vinyl alcohol), Poly(hydroxybutyrate).
Thermal Stabilizers	Benzofuranone, Pentaerythritol diphosphate (oxidative).
Compatibilizers	Polybutyrate, Acrylic acid, Benzene diboronic acid, Poly(caprolactone).
Impact Modifiers	Poly(ethylene glycol-oxide), Poly(caprolactone).
Flame Retardants	Ammonium polyphosphate, Phosphonate, Phosphine oxide, Natural fiber (NF), Fiber network fabric (FNF), Zinc borate.

1.5. Improvement of Thermal Degradation and Flame Retardant Characteristics of PLA

1.5.1. Thermal Stability of Polymers

“The thermal stability of polymers is dependent upon their constituent chemical bonds and the hydrogen transfer reactions within them. For instance, polymers containing aliphatic units undergo thermal degradation at lower temperatures compared to aromatic polymers because their C-C bonds are weaker and aliphatic hydrogen atoms are transferred more easily. In case of “high temperature” polymers the thermal stability is the result of the lack of movement of hydrogen atoms within the polymer structure, achieving a “quasi-char” structure in the synthetic stage. As a consequence, these polymers start decomposing at relatively high temperatures yielding large amounts of char” [32].

“A great difference exists between the mechanisms of thermal decomposition of addition polymers and condensation polymers. Addition polymers contain aliphatic hydrogen atoms along the backbone, which are easily mobilized after homolytic bond cleavage in the temperature range of 200–500°C. Most of the addition polymers undergo thermal degradation through the formation of macro-radicals, which are very reactive species. Their decay may happen through several parallel routes, involving bond cleavages (e.g., beta scission, recombination, disproportionation, hydrogen elimination or abstraction. Elimination of small stable molecules from side groups (e.g., HCl, H₂O) may play also a role” [32].

“Condensation polymers can be regarded as a sequence of monomer units containing functional groups immobilized into the polymer structure. Their decomposition pathways will be affected by the polarity and reactivity of the functional groups within their structure and the thermal decomposition reactions will be ionic and selective. The specific thermal decomposition pathways

occurring in condensation polymers largely depend upon the nature of the functional groups and the chemical structure of the monomer units. This situation causes drastic changes in pyrolysis mechanisms even within the same class of condensation polymers. These ionic pathways usually occur at temperatures (150–300°C) that are below those of typical free-radical degradation reactions. However, if these polymers are subjected to higher temperatures, radical reactions are likely to prevail. Furthermore, polymers containing less polar functional groups, like ethers and azomethynes, tend to undergo radical cleavage even at relatively low decomposition temperatures” [32].

1.5.2. Heat Stabilizers

Heat stabilizers are used to prevent oxidation of plastics by thermal processes, both in processing and usage. These stabilizers should be effective as long as the durability of the polymer itself. These materials should not leave the polymer structure during usage. It is also important that the stabilizer is well distributed in the polymer to function properly [30].

1.5.3. Flame Retardants

Flame retardants play an important role as additives for plastics. Many good examples exist where high performance plastics have found new applications in industrial markets. In recent years, some researchers have given much attention on producing fully biodegradable biocomposites by compounding natural fibers with biodegradable polymers. Compared to traditional composites, these biocomposites have many advantages over commercial polymers like biodegradability, lower density, higher tensile strength and modulus than common biodegradable polymers and lower costs. Biodegradable polymer

biocomposites have various applications such as automotive components, electrical and electronics, building materials, and the aerospace industry due to ecological and economical advantage over conventional composites [30].

However, there are still three factors limiting the applications of natural polymers in these fields: low compatibility with hydrophobic polymer matrices, thermal sensitivity during processing and flammability. As flammability conflicts with the safety requirements for many fields, the improvement of flame retardancy of biocomposites becomes a very important subject for biopolymer production. Two general approaches to achieve flame retardancy in polymers are known as the “additive” and the "reactive" types. Most common method used to achieve flame retardancy is the incorporation of flame-retardants into polymers. Flame retardants are materials which can interfere with the combustion during a particular stage of the process so that the material shows satisfactory flame retardancy [30].

1.5.3.1. Boron-Based Flame Retardants

Boron compounds are used for improvement of properties regarding to flammability, flame retardancy and thermal degradation of polymeric materials. The incorporation of boron into polymer matrices has gained importance in recent years as it improves thermal stability, electrical resistance, oxidative resistance flexibility and especially flame retardancy compared to the virgin polymer. Boron based flame retardants act mainly in the condensed phase by shunting the decomposition process into carbon formation rather than CO or CO₂ formation [33].

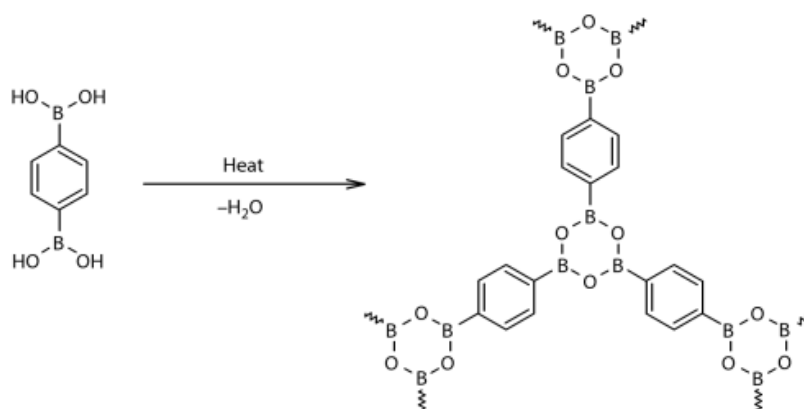
Boron compounds promote char formation which forms a protective layer/barrier to prevent oxidation of carbon in the burning process. The char formation relates to the thermal action of boronic acid with alcohol moieties. The main reason of significant improvement of flame retardancy is the mechanism

involving the formation of a protective barrier of boron oxide, which in turn prevents the degradation of the polymer. Among the boron based flame retardants, boronic acids are the most promising because of the formation of a boroxine network during heating. This structure contributes to the formation of char and prevent the fuel molecules being conveyed to the combustion surface [33].

This network also acts as a thermal insulator to protect the remaining unburned plastic from thermal degradation. This is mostly because the crosslinking results in a boronate glass structure [34]. In summary, these compounds can be used as reactive non-halogenated flame retardants [33].

1.5.3.2. Benzene-1,4-Diboronic Acid (BDBA)

Although boronic acid derivatives are not yet used as flame retardants, it has a good potential of commercialization [35]. Boronic acids release water on thermolysis, thereby leading to the formation of boroxines or boronic anhydrides. Boronic acid groups are considered as condensed phase flame retardants. They become active in condensed phase by assisting intermolecular cross-linking, and become good char-yielding compounds, forming a cross-linked boroxine network through the loss of water, as seen in Scheme 1.3 [35, 36].



Scheme 1.3. Formation of boroxine from para-diboronic acid [36].

1.5.3.3. Zinc Borate (ZnB)

“Zinc borate (ZnB) is one of the boron-containing flame retardants with the general formula of $x\text{ZnO}\cdot y\text{B}_2\text{O}_3\cdot z\text{H}_2\text{O}$. There exist several formulations for ZnB based retardants, depending on the reaction conditions. Some of the common formulations are shown in Table 1.2. $2\text{ZnO}\cdot 3\text{B}_2\text{O}_3\cdot 3.5\text{H}_2\text{O}$, $2\text{ZnO}\cdot 3\text{B}_2\text{O}_3$ and $4\text{ZnO}\cdot \text{B}_2\text{O}_3\cdot \text{H}_2\text{O}$ remain stable up to 290-300°C, to at least 500°C and to higher than 415°C, respectively” [37].

Table 1.2. Common ZnB formulations [37].

Formula	Trade Name
$2\text{ZnO}\cdot 3\text{B}_2\text{O}_3\cdot 7\text{H}_2\text{O}$	ZB-237
$2\text{ZnO}\cdot 2\text{B}_2\text{O}_3\cdot 3\text{H}_2\text{O}$	ZB-223
$2\text{ZnO}\cdot 3\text{B}_2\text{O}_3\cdot 3.5\text{H}_2\text{O}$	Firebrake ZB
$2\text{ZnO}\cdot 3\text{B}_2\text{O}_3$	Firebrake 500
$4\text{ZnO}\cdot \text{B}_2\text{O}_3\cdot \text{H}_2\text{O}$	Firebrake 415

Zinc borates act as flame retardant by forming char, decreasing the heat release rate, and preventing the emission of smoke, formation of carbon monoxide and afterglow combustion. They also exhibit synergistic effect in the presence of metal hydroxides. Moreover, it also acts as an anti-arcing agent [37].

1.5.3.4. Flame Retardancy of Polymer/ Layered Silicate Nanocomposites

The most significant effect of the addition of layered silicates in polymers by the formation of nanocomposites structure (intercalated and exfoliated) is the

reduction of peak heat release rate (PHRR) with respect to neat polymer matrix . In addition to the reduction of PHRR, the layered silicates increase the thermal stability and the char formation in a variety of polymers [38].

Formation of multilayered carbonaceous-silicate layer, a combination of physical and chemical processes, is the most important reason for the reduction of PHRR. The schematic view of the migration of the layered silicates is shown in Figure 1.1 [39].

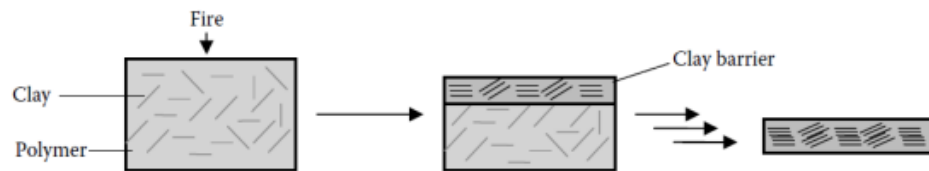


Figure 1.1. Schematic view of the migration of the layered silicates during burning [39].

According to previous studies, this carbonaceous-silicate layer acts as a barrier for mass and heat transport and slows down the burning rate during combustion. By the barrier effect of carbonaceous-silicate layer, the heat release rate of flammable fuel is reduced but the total amount of fuel source does not change, so the combustion continues until almost all the carbon mass has been pyrolyzed and combusted [40-45].

1.6. Reinforcement of PLA

Fibers are usually incorporated into polymeric materials to improve mechanical properties. Vegetable fibers are the most common bio-material used for reinforcement of PLA. Cellulose is the major constituent of vegetable fibers.

Cellulose fiber-reinforced polymers have gained some importance with the focus on renewable raw materials. There also exist some minerals which have a fibrous structure [46].

The reinforcement of polymers using fillers is common for the processing of polymeric materials. Nanoscale fillers gained some interest in the last two decades, as a relatively rigid nanostructure can be built from a polymer and a layered nanoclay. This new nanocomposite shows dramatic improvement in mechanical properties with low filler content [30].

The reinforcement of renewable polymers is highly important as these polymers have subpar properties compared to commercial polymers. Also, the hydrophilic behavior of natural polymers makes interfacing of the nanostructure much easier as filler [30]. Examples of usable materials for reinforcement of PLA, is given below:

Natural Fibers: Cellulosic fibre.

Fibrous/Layered Clays: Montmorillonite, mica, sepiolite.

Recently, PLA nanocomposites based on layered silicates has been actively investigated due to significant improvements over the virgin polymer in terms of mechanical, fire retardant, gas barrier and other properties [30].

Some examples of clay minerals used for modification are listed below:

Muscovite: A potassium-aluminum silicate mineral cleaves as tiny leaves promoting layered structure.

Kaolinite: An aluminum silicate mineral with layered structure composed of alternating tetrahedral and octahedral molecular structures.

Bentonite: This mineral is mostly composed of montmorillonite (impure form).

Montmorillonite: A smectite group mineral consisting of aluminum-magnesium silicate with layered structure (2 tetrahedral + 1 octahedral layer structure).

1.6.1. Improvement of Properties of PLA via Montmorillonite (MMT)

The thermal, mechanical, fire retardant and gas barrier properties of PLA can potentially be improved by adding organically modified clays such as smectite and mica into the polymeric matrix [30]. But the modification can cause a tradeoff, such that; while improving the mechanical properties, it could interfere with the thermal properties (lower stability) of the material [47]. Also, the amount of additive loaded into the polymer matrix affects the properties of the final nanocomposite [48].

Recent developments of high-performance additives address more complex or newer requirements, more stringent processing/usage conditions and/or environmental concerns, nevertheless the primary objective still is maintaining polymer properties. In near future, there will be added effects and functionalities into polymers by additives which would result in several innovations in the polymer industry [30].

1.6.1.1. Structure and Properties of Montmorillonite (MMT)

“Montmorillonite (MMT) is one of the most commonly used layered silicates. Layered silicates used for the preparation of polymer layered silicate (PLS) nanocomposites belong to the same general family of 2:1 layered of phyllosilicates. Their crystal structure consists of layers made up of two tetrahedrally coordinated silicon atoms fused to an edge-shared octahedral sheet of either aluminum or magnesium hydroxide. The layer thickness is around 1 nm, and the lateral dimensions of these layers may vary from 30 nm to several

microns or larger, depending on the particular layered silicate. Stacking of the layers leads to a regular van der Waals gap between the layers called the interlayer or gallery. Isomorphic substitution within the layers (for example, Al^{3+} replaced by Mg^{2+} or Fe^{2+} , or Mg^{2+} replaced by Li^{1+}) generates negative charges that are counter balanced by alkali and alkaline earth cations situated inside the galleries. This type of layered silicate is characterized by a moderate surface charge known as the cation exchange capacity (CEC), and generally expressed as meq/100 gm. This charge is not locally constant, but varies from layer to layer, and must be considered as an average value over the whole crystal” [19].

Layered silicates have two types of structure: tetrahedral-substituted and octahedral substituted. In the case of tetrahedrally substituted layered silicates the negative charge is located on the surface of silicate layers, and hence, the polymer matrices can interact more readily with these than with octahedrally substituted material. Details regarding the structure for these layered silicates are provided in Figure 1.8.

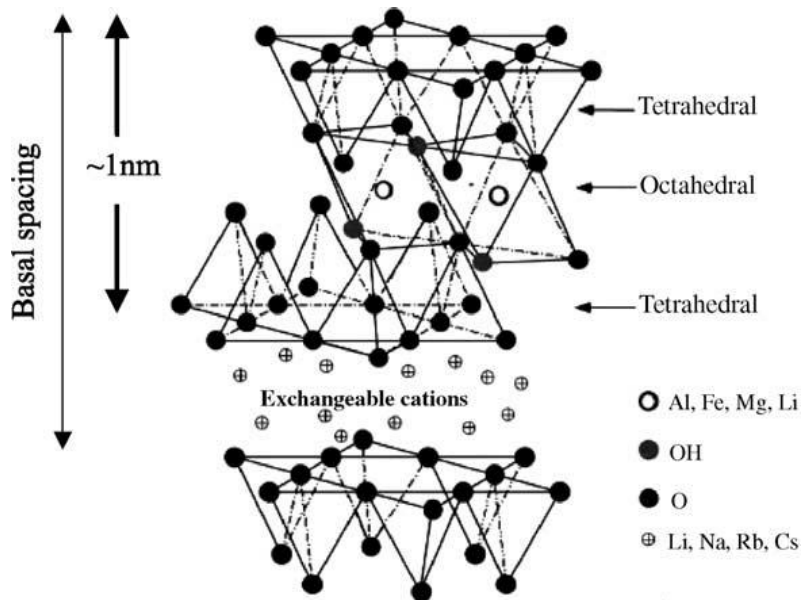


Figure 1.8. Structure of 2:1 phyllosilicates [19].

MMT, as an example for 2:1 layered phyllosilicates has a general formula of $M_x(\text{Al}_{4-2x}\text{Mg}_x)\text{Si}_8\text{O}_{20}(\text{OH})_4$ where M stands for monovalent cation and x is degree of isomorphous substitution between 0.5 and 1.4. It has a cation exchange capacity of 100meq/100g and particle length is 100-150 nm [19].

1.6.1.2. Modification of MMT

Production of PLA nanocomposites is affected by two particular characteristics of layered silicates. The first is the ability of the silicate particles to disperse into individual layers. The second characteristic is the ability to fine-tune their surface chemistry through ion exchange reactions with organic and inorganic cations. These two characteristics are interrelated since the degree of dispersion of layered silicate in a particular polymer matrix depends on the interlayer cation [19].

Organoclays are mostly prepared by modifying the montmorillonite clay with quaternary amines (long chain). The nitrogen end of the quaternary amine is positively charged, and attacks the sodium or calcium ion in the mineral structure. After this modification process, the clay becomes hydrophobic utilizing certain amines that are organophilic [49].

1.7. Preparation of PLA Nanocomposites

Polymer nanocomposites based on thermoplastic matrices could be prepared by three different methods:

- a) **In-Situ Polymerization:** Dispersed nanoclay is incorporated into the monomer followed by polymerization.
- b) **Solution Intercalation:** Nanoclay is mixed with the polymer in solution and followed by solvent evaporation.

c) **Melt Compounding:** The nanoclay is blended with the polymer in the molten state [30].

“Melt compounding is the simplest and most common method for industrial applications because of solvent absence and compatibility with common mixing and processing equipment and techniques. In this approach, the polymer and nanoparticles are generally blended through a twin-screw extruder at a temperature above the polymer melting point. Under the right conditions, the stress applied during mixing may result in the diffusion of the polymer chains from the bulk into the gallery spacing of the clay, and formation of an intercalated or exfoliated structure, depending on the penetration of polymer. Although the mechanical, barrier properties and biodegradability of PLA can potentially be improved by adding organically modified clays into the polymeric matrix, thermal degradation of PLA appears to be adversely effected by clay incorporation, resulting in a loss of molecular weight. Considering that the rate of thermal degradation increases after clay loading, mitigation of the thermal degradation in PLA nanocomposites is a crucial problem for clay based modification process” [29].

For some applications, PLA needs modification. High stiffness and brittleness at ambient temperature or below could be improved by blending the polymer with a biodegradable plasticizer. However, some properties like the tensile strength, thermal stability and gas barrier properties of the resulting polymer still needs to be improved to fulfill the requirements for specific applications (e.g. food packaging) [30].

1.8. Boron Compounds and Nanoclay Containing PLA Composites

Inclusion of small amounts of nanoclay into PLA resulted reduction of flammability of composites according to previous studies [50-52]. Synergistic

effect was observed as C30B nanoclay incorporated to PLA [53]. Zhan et al. stated that the addition of nanoclay and zinc borate into PLA increased the LOI values of composites. They also performed UL-94 test and nanoclay and zinc borate exhibited as good anti-dripping agent according to test results [54]. Nanoclay addition generally caused reduction in heat release rate and increasing in char formation for polymer nanocomposites [39, 55, 56]. Previous studies show that nanoclay does not affect much UL-94 ratings and LOI values of polymers unless they used as a synergetic agent with other flame retardants [39, 57-59].

Effects of nanoclay to mechanical properties of PLA composites have been investigated by several researchers. Krishnamachari et al. found that tensile strength and Young's modulus of PLA were enhanced with the addition of Cloisite 30B with 1% content [60]. According to Zaidi et al., incorporation of Cloisite 30B into PLA matrix caused reduction of tensile strength and improvement in modulus [61].

Influence of nanoclay addition to thermal degradation of PLA was also studied in academic field. In these works it was concluded that Cloisite 30B filled PLA thermally degraded more easily as compared to similar nanoclay types [62, 63].

Wootthikanokkhan et al. studied thermomechanical properties of PLA/Cloisite30B which were prepared by using melt mixing method. They found that percent crystallinity and modulus of composites increased where tensile strength and strain values drop down after addition of nanoclay [64].

DSC technique is widely performed for the aim of investigation thermal behaviors of polymer/MMT nanocomposites [65]. In the work by Tian and Tagara, effect of preparation route of PLA/MMT nanocomposites to polymer morphology is studied. DSC analysis showed that change in melting enthalpy of nanocomposites was higher in the case of melt-blending method [66].

Boric acid derivatives and zinc borates were used as flame retardants in several studies by the aim of halogenated fire retardant replacement [67-69]. It was shown that the boronated PS is significantly less flammable than the unmodified PS as it has a LOI of 13.3% while the boronated PS has 25.3% (degree of substitution: 9.2%). The char yield also increased from <1% to 7% at 600°C [35, 36].

Evaluation of 1,4-benzenediboronic acid (BDBA) and 1,3,5-benzene-triboronic acid (BTBA) as fire retardants for ABS and PC by using TGA and DSC analysis showed that both compounds have an endothermic event in the range of 180°C-260°C. The char yields obtained for BDBA and BTBA at 900°C were 40% and 48 % respectively [36]. An increase in boron concentration also lowers the heat released from the polymer due to the formation of a glassy intumescent that hinders the heat transfer [35].

1.9. Objective of This Thesis

In this study, the effects of addition of different types and amounts of boron compounds and the reinforcement material are investigated over the morphological, thermal and mechanical behavior of poly(lactide) (PLA). By this aim, two different boron compounds (zinc borate and benzene-1,4-diboronic acid) and methyl tallow bis-2-hydroxyethyl ammonium modified montmorillonite Cloisite 30B (C30B) are used for preparation of different poly(lactide) (PLA) composites.

For this purpose, for morphological analyses X-Ray Diffraction (XRD), Transmission Electron Microscope (TEM), Scanning Electron Microscope (SEM) techniques, for thermal analyses, Thermogravimetric Analysis (TGA), Differential Scanning Calorimetry (DSC), and Direct Pyrolysis Mass Spectrometry (DP-MS) techniques, for flame tests Underwriters Laboratory UL 94 Test (UL-94) and limiting oxygen index (LOI) tests and finally for mechanical analyses tensile tests are applied.

CHAPTER 2

EXPERIMENTAL

Experimental section is divided into three subsections. In the first part, the materials used for preparation of composite materials will be given. In the second part, the method and preparation of different polymer composites are stated. In the last part, the characterization techniques used for investigation of mechanical, thermal and flame retardancy properties of polymer composites are explained.

2.1. Materials Used for Preparation of Nanocomposites

Poly lactide, PLA, ($M_n \sim 190000$), was acquired from Cargill Dow LLC.

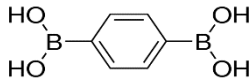
Methyl tallow bis-2-hydroxyethyl ammonium modified montmorillonite Cloisite 30B (C30B) was used as reinforcement material and purchased from Southern Clay Products Inc. The specifications of organically modified Cloisite 30B is stated in Table 2.1.

Table 2.1. Specifications of organically modified Cloisite 30B.

Montmorillonite	d_{001} (nm)	Amount of organic modifier	Organic modifier
Cloisite 30B	1.85	90 meq/100g clay	$\begin{array}{c} \text{CH}_2\text{CH}_2\text{OH} \\ \\ \text{H}_3\text{C}-\text{N}^+-\text{T} \\ \\ \text{CH}_2\text{CH}_2\text{OH} \end{array}$

Firebrake ZB type Zinc Borate was supplied from Luzenac Group. Parabenzene-dibronic acid, BDBA was purchased from Sigma-Aldrich Co. Specifications of boron compounds used are given in Table 2.2.

Table 2.2. Specifications of boron compounds.

Material	Supplier	Composition / Chemical Formula	Specifications
ZnB (Firebrake ZB)	Luzenac Group	ZnO (37.7-38.7%), B ₂ O ₃ (47.5-48.9%), H ₂ O (12.4-14.8%).	Appearance: White Powder Density: 2.77 g/cm ³ Particle size: 9 μm
BDBA, 1,4-	Sigma-Aldrich Co.	C ₆ H ₄ [B(OH) ₂] ₂	Structure:  Purity: ≥ 95.0%

2.2. Preparation of Nanocomposites

In this study, melt blending technique was applied for preparation of different composite materials. PLA matrix, boron compounds and Cloisite 30B were dried at 65 °C overnight under vacuum before extrusion process for melt blending.

2.2.1. Melt Blending Method

Melt mixing of PLA with ZnB, or 1,4- BDBA boron compounds and 3 wt. % C30B was carried out using a DSM Xplore twin screw micro compounder. After pre-mixing the mixture was fed continuously into the mixing unit of the extruder and mixed for 8 min at 190 °C at a constant screw speed, 100 rpm. The compositions of the melt blends prepared are summarized in Table 2.3.

Table 2.3. Composition of PLA nanocomposites prepared by melt blending technique.

Samples	wt. % of Compound			
	PLA	ZnB	BDBA	C30B
PLA	100	-	-	-
PLA-1ZnB	99	1	-	-
PLA-2ZnB	98	2	-	-
PLA-3ZnB	97	3	-	-
PLA-1ZnB-NC	96	1	-	3
PLA-2ZnB-NC	95	2	-	3
PLA-3ZnB-NC	94	3	-	3
PLA-1BDDA	99		1	-
PLA-2BDBA	98		2	-
PLA-3BDBA	97		3	-
PLA-1BDBA-NC	96		1	3
PLA-2BDBA-NC	95		2	3
PLA-3BDBA-NC	94		3	3

Here, NC refers 3% C30B addition.

2.2.1.1. Extrusion

The mixing of PLA, boron compounds and nanoclay (C30B) at various composition ratios was carried out using counter rotating twin screw microextruder (15 ml microcompounder®, DSM Xplore, Netherlands) at 100 rpm at 190 °C for 8 minutes.

2.2.1.2. Compression Molding

In this study, compression molding was applied to obtain LOI and UL-94 test samples. Firstly, the material to be molded was preheated in a heated, open mold cavity. Then, the cavity was closed and the sample was heated under high pressure. After the molding process was completed, the sample was cooled and removed.

2.2.1.3. Injection Moulding

For the mechanical tests, melt mixed samples were dried at 65 °C for 2 hours prior to shaping processes. Nanocomposites were shaped to the “dog-bone” structure, by the usage of Daka Injection Molding Instrument, as illustrated in Figure 2.2. All of the dog-bone shaped specimens had identical length (L), width (W), and thickness (T) as 50 mm, 7.6 mm, and 2 mm, respectively.

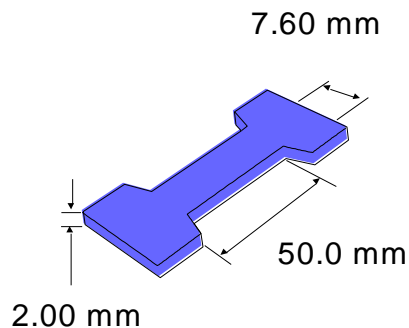


Figure 2.2. Schematic representation of dog-bone specimen.

During the process, the specimens for mechanical tests were molded by a laboratory scale injection-molding machine (Microinjector, Daca Instruments) at a barrel temperature of around 190-195 °C, and the mold temperature of 40 °C. Extruded nanocomposites were forced to mold cavities at 8 bar pressure.

2.3. Apparatus Used for Characterization Techniques

The structural, morphological, thermal, mechanical and fire properties were investigated by application of different techniques.

2.3.1. Structural & Morphological Analysis

2.3.1.1. X-ray Diffractometer (XRD) Analysis

Rigaku X-ray diffractometer (Model, Miniflex) with CuK α (30 kV, 15 mA, $\lambda = 1.54051 \text{ \AA}$) was used to obtain 2θ XRD patterns of the composites, at a scan rate of 1°/min over the range of $2\theta = 1^\circ$ -10°. X-ray analyses were performed at room temperature to injection molded dog bone shaped specimens.

2.3.1.2. Transmission Electron Microscope (TEM)

TEM analyses were carried out using a FEI Tecnai G2 Spirit BioTwin CTEM on the tensile fractured point of the specimens.

2.3.1.3. Scanning Electron Microscope (SEM)

Microstructures of the composites were analyzed by using QUANTA 400F Field Emission scanning electron microscope.

2.3.2. Thermal Analysis

2.3.2.1. Differential Scanning Calorimeter (DSC) and Thermogravimeter (TGA)

DSC and TGA analyses were conducted with a Perkin Elmer Instrument STA6000 device under inert environment supplied by continuous nitrogen flow at a flow rate of 20 mL/min, by heating the sample from room temperature to 500 °C at a heating rate of 10°C/min.

2.3.2.2. Direct Pyrolysis Mass Spectrometer (DP-MS)

2 µL solutions prepared by dissolving 0.10 mg PLA composites in chloroform, were injected into the flared glass sample vials. After the solvent was evaporated at room temperature, the samples were placed into the direct insertion probe. DP-MS analyses were performed on a 5973 HP quadruple mass spectrometry system coupled to a JHP SIS direct insertion probe pyrolysis system. 70 eV EI mass spectra, at a rate of 2 scan/s, were recorded during the pyrolysis. Samples were heated to 450°C at a rate of 10 °C/min. Experiments were repeated at least twice to ensure reproducibility.

2.3.3. Flammability Tests

2.3.3.1. UL- 94

UL-94 rating was obtained according to ASTM D3801 where V0 indicates the best flame retardancy and V2 is the worst. Bar specimens of 130 × 13 × 3.25 mm³ were tested.

2.3.3.2. LOI

LOI value was measured by using Dynisco Limiting Oxygen Index Analyzer instrument on test bars of size $130 \times 6.5 \times 3.25 \text{ mm}^3$, according to the standard oxygen index test ASTM D2863.

2.3.4. Mechanical Analysis

2.3.4.1. Tensile Test

Mechanical tests were performed with Lloyd LR 30 K universal tensile testing machine according to ASTM D638 standards. Tensile test machine worked with 5 cm/min crosshead speed and the cell load was 5 kN.

After extrusion, the substances were prepared for injection molding process and the dog bones obtained after injection were dried at 65 °C overnight under vacuum before tensile testing.



CHAPTER 3

RESULTS AND DISCUSSION

The morphological, mechanical, thermal properties and flame retardancy of the nanocomposites involving organically modified montmorillonite, Cloisite 30B and boron compounds, prepared by melt blending technique, were analyzed systematically and the amount of and the type of boron compound and also the effect of organically modified montmorillonite, Cloisite 30B were investigated.

3.1. Morphological Analysis

For morphologic analyses X-Ray patterns, TEM images of melt blended composites and SEM images of solution mixed composites were used.

3.1.1. Scanning Electron Microscope (SEM)

After the tensile analysis of dog bone shaped samples, the morphology of the tensile fractured surfaces of the samples were investigated through SEM images. Selected SEM images of melt blends, involving 1, 2, 3 wt. % ZnB, are shown in Figure 3.1.

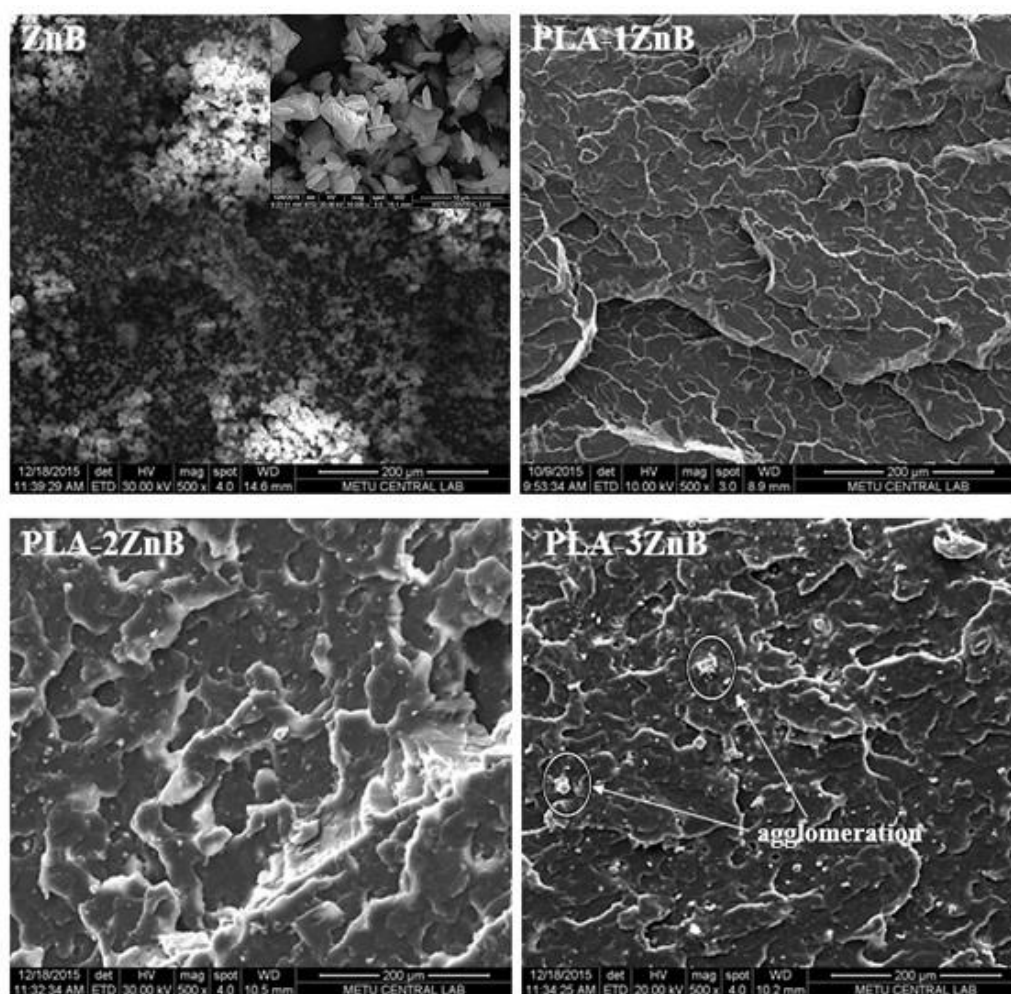


Figure 3.1. SEM images of ZnB and PLA-ZnB composites with 1%, 2% and 3% concentrations of ZnB at x500 magnification.

As seen in Figure 3.1, it can be noticed that ZnB is well-dispersed through the PLA matrix for 1 and 2 % concentrations. Agglomerates can be observed from the SEM micrograph of 3% ZnB containing composite.

Selected SEM images of melt blends, involving 1, 2, 3 wt. % BDBA, are shown in Figure 3.2.

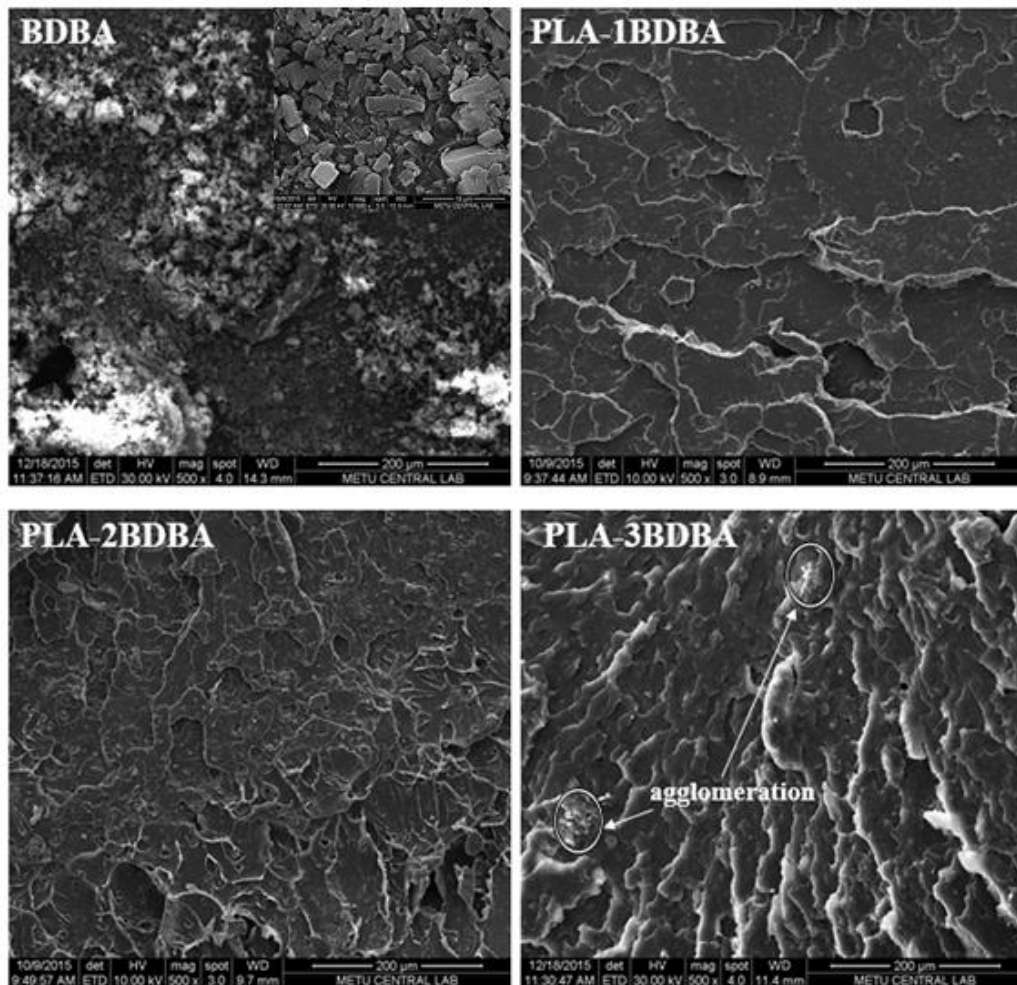


Figure 3.2. SEM images of BDBA and PLA-BDBA composites with 1%, 2% and 3% concentrations of BDBA at x500 magnification.

Homogenous dispersion is observed for PLA matrix involving 1% BDBA (Figure 3.2). Formation of agglomeration starts when the percent of BDBA is increased to 2 and agglomeration increases further upon addition of 3% BDBA.

3.1.2. Transmission Electron Microscope (TEM)

TEM images of PLA-ZnB and PLA-BDBA nanocomposites are shown in Figure 3.3. In the figures, the gray areas indicate the nano clay layers in PLA matrix which can be seen as the bright fields.

Although, some tactoid formations are visible, in general, dispersion of nanoclay in PLA-boron compound matrixes is observed. Higher magnification (50 nm) indicates more homogenous dispersion for the PLA-ZnB composite. Nanoclay shows intercalated structures and partially exfoliated regions are observable at higher magnifications.

In Figure 3.3, the dark entities indicate the cross-section of intercalated or stacked clay layers of BDBA containing composites. The stacked nanoclay layers are rarely seen due to agglomeration of nanoclay particles as observed in the general view. The TEM images with higher magnification (100 nm) indicate that nanoclay particles are well separated in the PLA-BDBA composite and are partially exfoliated in some areas, but not that much dispersed as in case of ZnB. These observations reveal that the type of the additive present in the matrix affects the nanoclay dispersion.

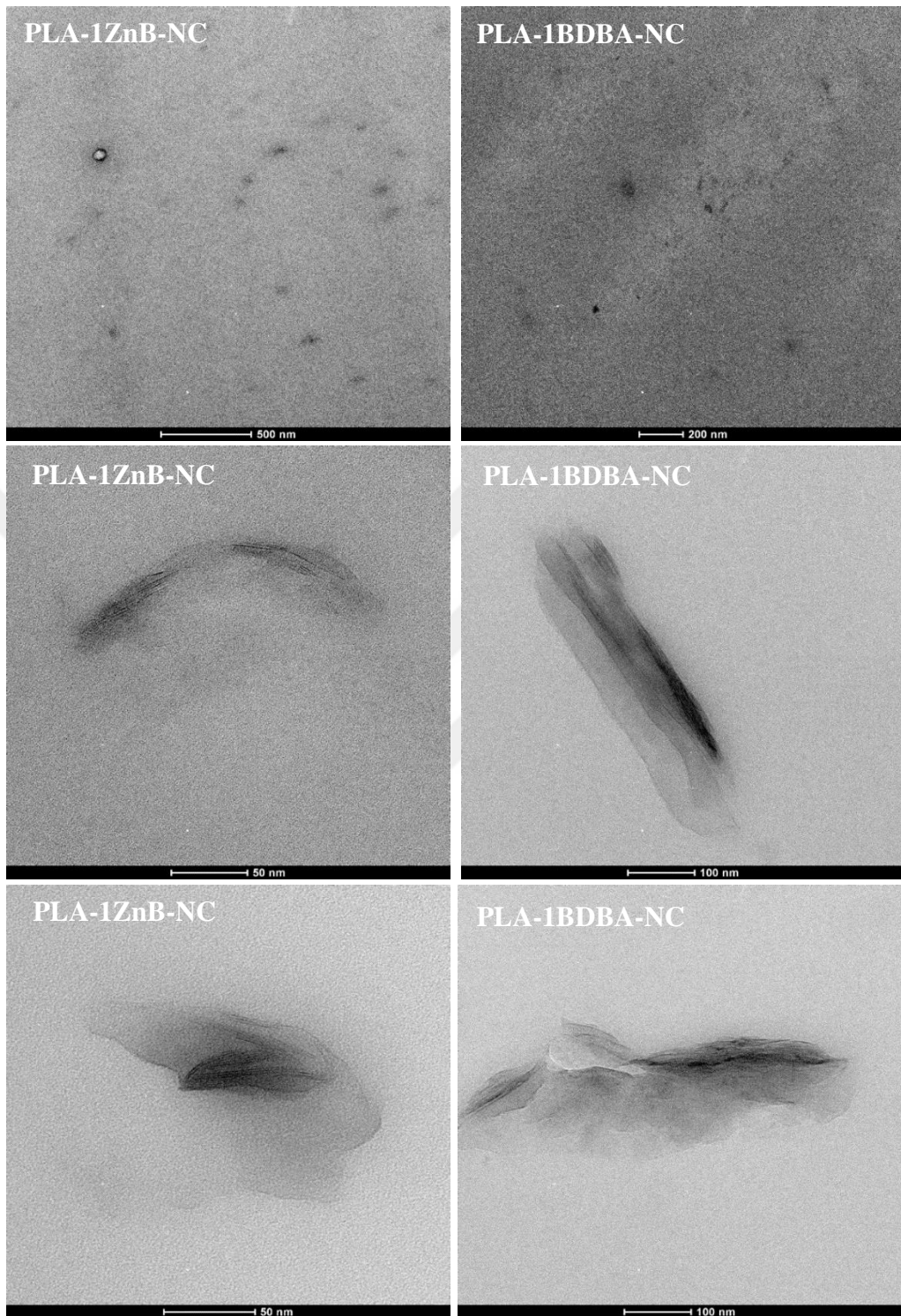


Figure 3.3. TEM images of 3% nano clay containing PLA-ZnB and PLA-BDBA composites at low (x1000) and high (x10,000) magnifications.

3.1.3. X-Ray Diffractometer (XRD)

As seen in Figure 3.4, crystalline peak of PLA is shifted to left and intensity of the broad peak is suppressed, whereas, those of ZnB are disappeared in the XRD diffractogram of PLA-ZnB with the addition of ZnB. In some areas, peaks belong to ZnB are seen in XRD diffractograms of composites, however those peaks are like noise and not significant. So, it may be said that ZnB is well dispersed in PLA matrix.

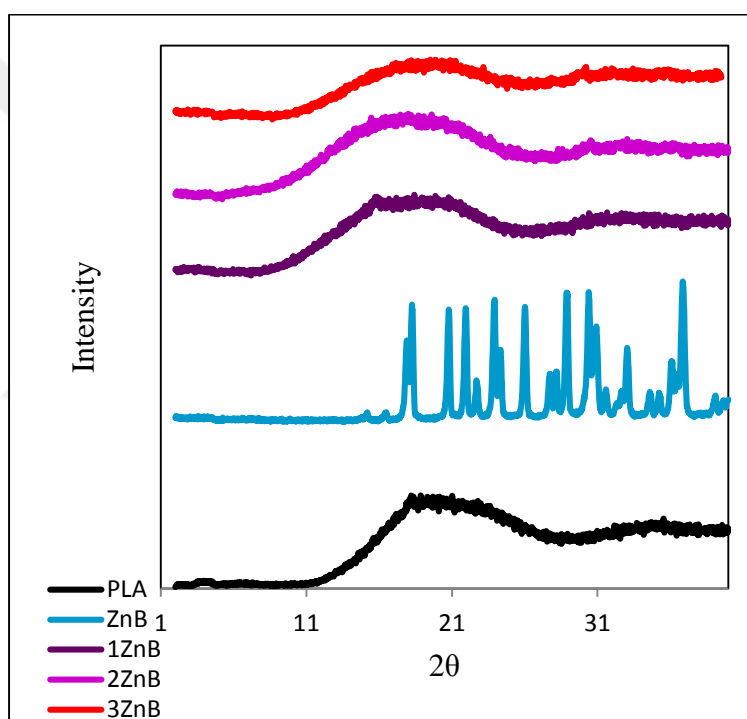


Figure 3.4. XRD patterns of neat PLA, ZnB and PLA-ZnB composites at different concentrations.

Similarly, the broad peak of PLA is suppressed with inclusion of BDBA as can be seen in Figure 3.5. Again, the crystalline structure of BDBA is lost in the PLA matrix. However, the intense peak of BDBA becomes visible in XRD pattern for 3% BDBA inclusion to PLA.

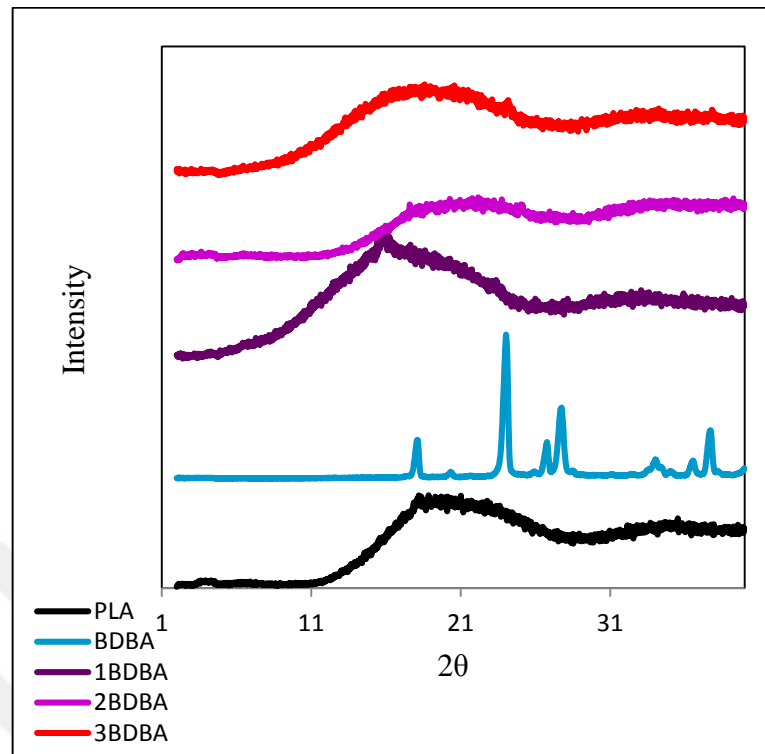


Figure 3.5. XRD patterns of neat PLA, BDDBA and PLA-BDDBA composites at different concentrations.

For determination of the dispersion of nanoclays and the exact structure of composites, TEM images should be evaluated together with XRD analyses of the tensile fractured samples involving nanoclay. XRD diffractograms are used for classification of composites as intercalated or exfoliated structures with respect to d-spacing measurements. Basically, if the ordered layers of a montmorillonite do not preserve their original spacing and increase as in the case of intercalated nanocomposites, the corresponding Bragg peak of nanoclay shifts to lower 2θ values. On the other hand, if the clay layers are either well separated/exfoliated from each other the Bragg peak no longer exists in the XRD diffractogram.

XRD patterns of PLA, NC, and PLA- NC composites involving 1, 2 or 3 % ZnB are shown in Figure 3.6. The diffractogram for nanoclay has a distinct maximum around $2\theta = 4.8^\circ$. This maximum peak is not observed for the ZnB and NC containing composites. This feature is characteristic of a good dispersion of the nanoclay. Observation of mainly intercalated structure is also in accordance with the TEM micrographs (Figure 3.3) of PLA-ZnB-NC composite, achieved by intercalation and partially exfoliation of the nanolayers in the PLA matrix, based upon the dispersion of nanoclays.

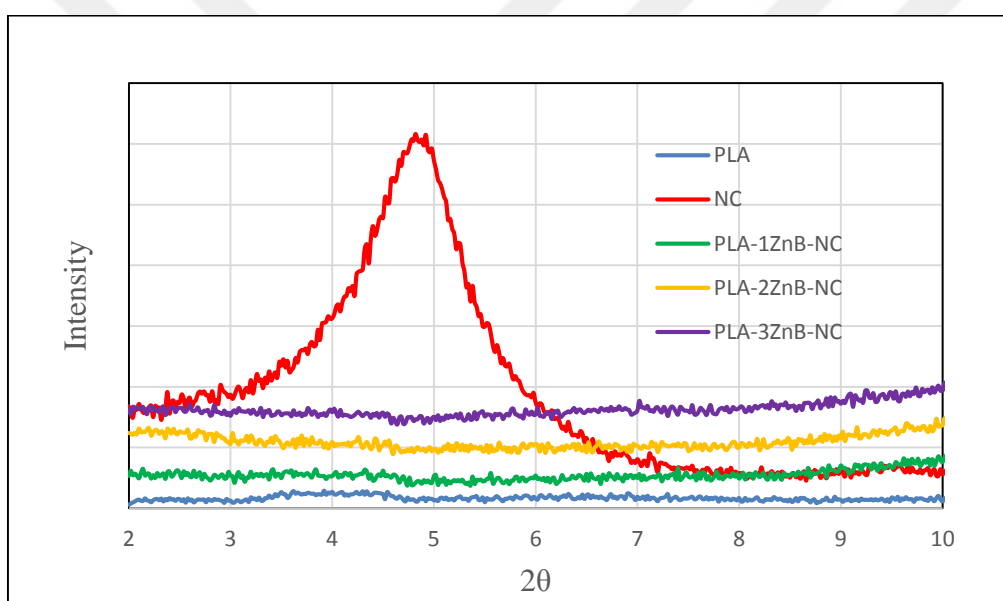


Figure 3.6. XRD patterns of neat PLA, nanoclay and PLA-ZnB-NC composites.

XRD of PLA, NC, and PLANC composites involving 1, 2, and 3 % BDBA are given in Figure 3.7. The characteristic peak ($2\theta = 4.8^\circ$) of Cloisite 30B also disappears in the diffractograms of BDBA and NC containing composites. The disappearance of corresponding Bragg peaks of montmorillonite indicates exfoliated dispersion in accordance. However, the TEM micrographs of PLA-

BDBA-NC composite (Figure 3.3), indicate that the exfoliated dispersion is not achieved properly. However, intercalated dispersion is observed clearly based upon the dispersion of nanoclays.

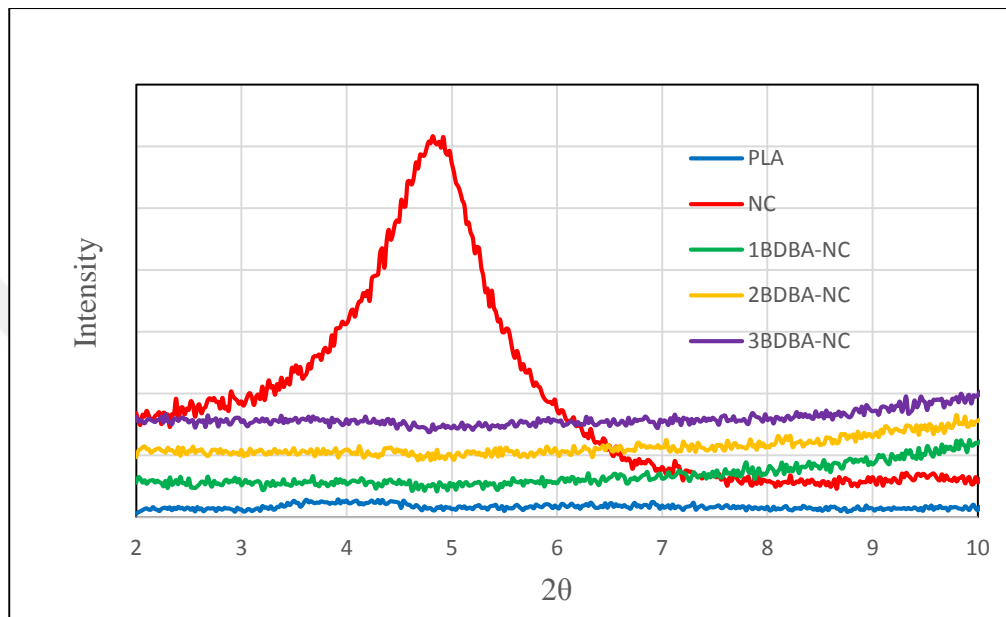


Figure 3.7. XRD patterns of neat PLA, nanoclay and PLA-BDBA-NC composites.

3.2. Thermal Analyses

Thermal characteristics of the composites were investigated via DSC, TGA and DP-MS techniques.

3.2.1. Differential Scanning Calorimetry (DSC) Analyses

For the investigation of thermal properties of neat PLA, PLA with boron compounds and PLA-boron compounds-nanoclay nanocomposites, various techniques including DSC were used.

In Figure 3.8 and 3.9, DSC thermograms of PLA involving different types and variable amounts of boron compounds and also nanofiller are given. With the addition of filler, crystallization temperature (T_c) peaks are shifted to left, so crystallization temperatures are effected. It may be concluded that due to the nanofiller-induced nucleating effect indicating generation of crystalline structures [72-75]. Melting temperatures of composites are shifted to slightly higher values upon incorporation of both ZnB and BDBA [72-75]. Inclusion of ZnB and BDBA into PLA shifts the glass transition temperature (T_g) to slightly lower temperatures. Similar results are observed in previous studies [72, 79].

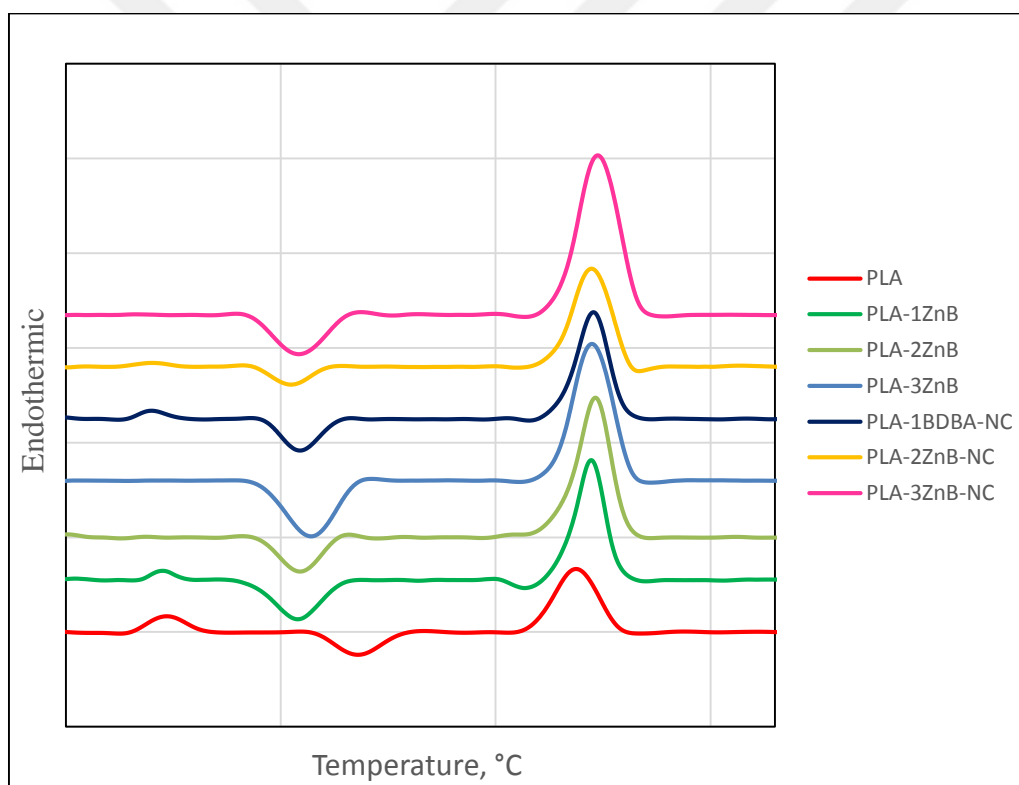


Figure 3.8. DSC thermograms of neat PLA, PLA involving variable amounts of ZnB (1, 2, 3 wt. %) and PLA-ZnB composites containing 3% wt. Cloisite 30B.

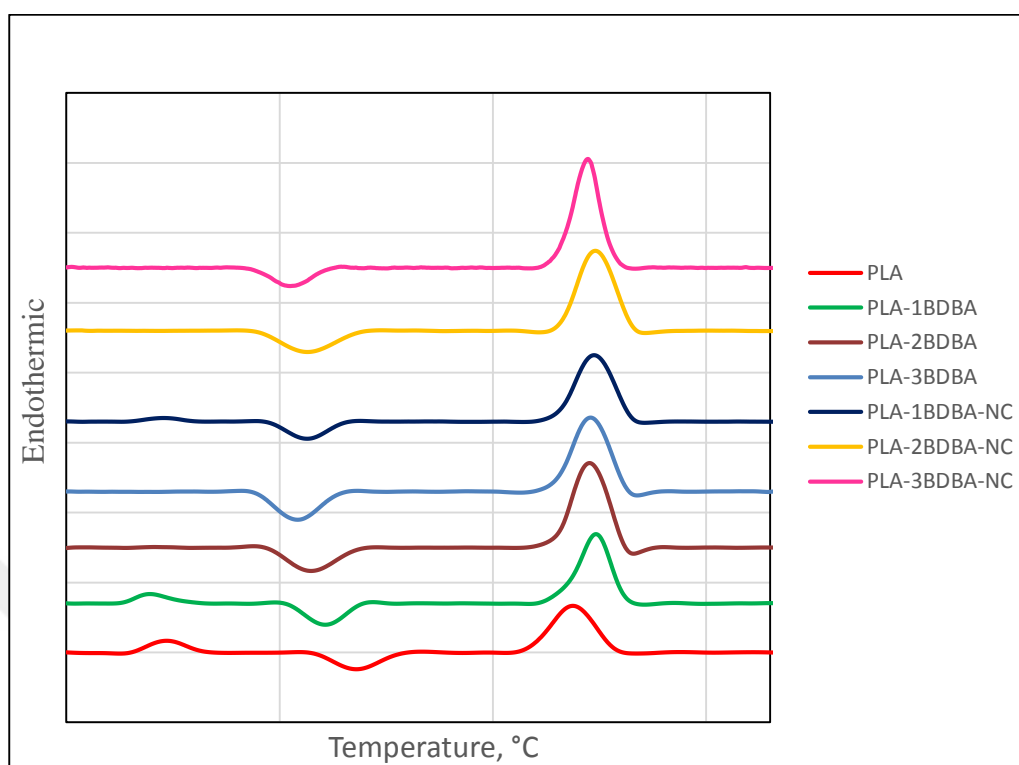


Figure 3.9. DSC thermograms of neat PLA, PLA involving variable amounts of BDBA (1, 2, 3 wt. %) and PLA-BDBA composites containing 3% wt. Cloisite 30B.

DSC results are given in Table 3.1. The increase in the amount of boron compounds added does not affect the melting temperatures significantly. It is also observed from the DSC results that, addition of any filler causes nearly negligible change in T_g of polymer, but T_c values decreases significantly due to nucleating effect of nanofiller.

Table 3.1. DSC test results of neat PLA, PLA involving variable amounts of boron compounds and PLA-boron composites containing 3% wt. nanoclay.

Samples	DSC results		
	T _g (°C)	T _c (°C)	T _m (°C)
PLA	65.4	114.1	165.1
PLA-1ZnB	65.1	100.7	168
PLA-2ZnB	60.1	100.0	168.6
PLA-3ZnB	61.4	102.3	168.4
PLA-1ZnB-NC	60.4	100.7	169.3
PLA-2ZnB-NC	61.1	98.2	169.1
PLA-3ZnB-NC	61.7	99.4	170.2
PLA-1BDDA	63.2	106.2	170.6
PLA-2BDBA	62.6	103.4	168.4
PLA-3BDBA	61.8	99.8	168.5
PLA-1BBDA-NC	64.0	106.2	170.0
PLA-2BDBA-NC	60.2	105.6	169.5
PLA-3BDBA-NC	58.9	98.7	167.0

3.2.2. Thermogravimetric (TGA) Analyses

TGA data for PLA composites containing boron compounds with different compositions and PLA-boron composites with nanoclay are summarized in Table 3. 2, and TGA curves of all composites prepared are shown in Figure 3.10.

The inclusion of ZnB to PLA slightly increases the char yield from 0.36 to 2.13 % for the highest concentration (Table 3.2). Addition of BDBA into PLA increases the char yield slightly from 0.36 to 0.73. Inclusion of nanoclay significantly increase the char yield for both of the composites. At elevated temperatures, presence of nanoclay promotes char formation [80]. Both $T_{5\%}$ and T_{max} values are shifted to low temperatures upon additions of boron compounds into PLA matrix (Table 3.2). The reductions are more significant for ZnB filled composites, in other words, ZnB destabilizes the PLA.

Upon incorporation of nanoclay into PLA/boron compound matrix, the char yield is slightly increase, however, no noticeable effect on the thermal behavior is recorded.

Table 3.2. TGA data for PLA, PLA/boron compounds with or without 3% C30B.

	wt. % of compound	wt. % C30B	T _{5%} , °C	T _{10%} , °C	T _{max} , °C	% char yield
PLA			323.4	332.4	355	0.36
PLA-ZnB	1	-	295.1	302.6	328.4	1.75
	2	-	300.0	307.7	337.5	1.83
	3	-	295.1	302.3	330.4	2.13
PLA-ZnB-NC	1	3	294.4	303.8	336.5	2.35
	2	3	296.7	305.2	336.5	2.53
	3	3	296.1	305.1	333.5	3.88
PLA-BDBA	1	-	304.5	314.4	349.3	0.63
	2	-	308.1	319.8	345.3	0.68
	3	-	302.4	315.2	352.6	0.73
PLA-BDBA-NC	1	3	297.8	308.3	355.2	1.56
	2	3	300.7	314.4	354.8	1.89
	3	3	293.2	307.5	354.6	2.50

As can be observed in Figure 3.10-a, nanoclay addition causes slight reduction on decomposition rate of ZnB and BDBA containing composites at their lowest concentration (1%). However, as shown in Figure 3.10-c increase in decomposition rate and char yield is observed for nanoclay containing composites of boron compounds at their highest concentration (3 %).

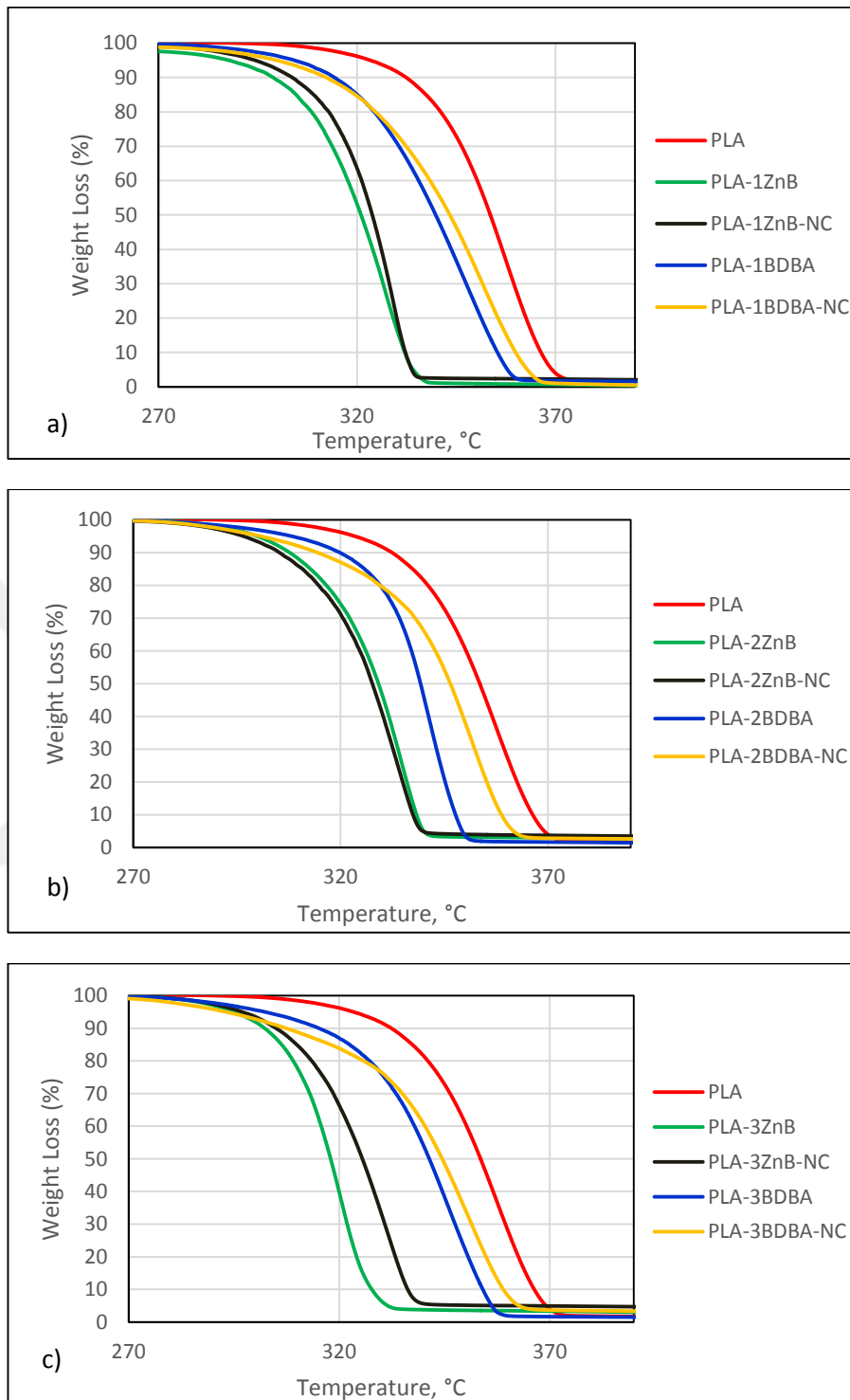


Figure 3.10. TGA curves of PLA composites containing boron compounds with different compositions and PLA-boron composites with nanoclay addition.

3.2.3. Direct Pyrolysis Mass Spectrometry (DP-MS) Analyses

In order to determine the effects of boron compounds on thermal degradation of PLA and PLA-NC composites, the pyrolysis mass spectrometry analyses of each component and composites involving different amounts of boron compounds are performed and compared.

3.2.3.1. PLA

The total ion current, TIC, curve (the variation of total ion yield as a function of temperature), the pyrolysis mass spectrum recorded at the maximum of the TIC curve, at 368°C during the pyrolysis of PLA are given in Figure 3.11. The base peak is at $m/z=200$ Da is attributed to $(C_2H_4CO_2)_2C_2H_4CO$. The spectrum is dominated by the known homologous series of peaks at $m/z=(72x-88)$ Da for $x=2$ to 9 associated with $(C_2H_4CO_2)_xC_2H_4CO$ for $x=0$ to 9, fragments that are produced by elimination of the neutral molecules, CO_2 and acetaldehyde during ionization of the cyclic oligomers, $(C_2H_4CO_2)_x$. Molecular ions of cyclic oligomers generated by inter and/or intra trans-esterification reactions during the thermal degradation of PLA are not stable even if they are produced with the soft ionization techniques. Peaks due to low mass fragments such as CH_3CHO (56 Da), CO_2 (44 Da), CO and/or C_2H_4 (28 Da) are associated with random chain cleavages. Series of peaks with $m/z=(72x+73)$ Da for $x=0$ to 9, due to fragments produced by cis-elimination reactions, with general formula $(C_2H_4CO_2)_xH$ (for $x=1$ to 10) are also detectable yet, less pronounced. The reaction mechanisms for thermal degradation are summarized in Scheme 3.1. Random chain scissions along the polymer backbone are including many α -cleavages of polyesters is shown in Scheme 3.1-a. Depolymerization of cyclic lactide oligomers by back-biting (intramolecular trans-esterification reaction) is shown in Scheme 3.1-b. Cis-elimination reactions are also important leading to the formation of olefinic double bond (Scheme 3.1.-c).

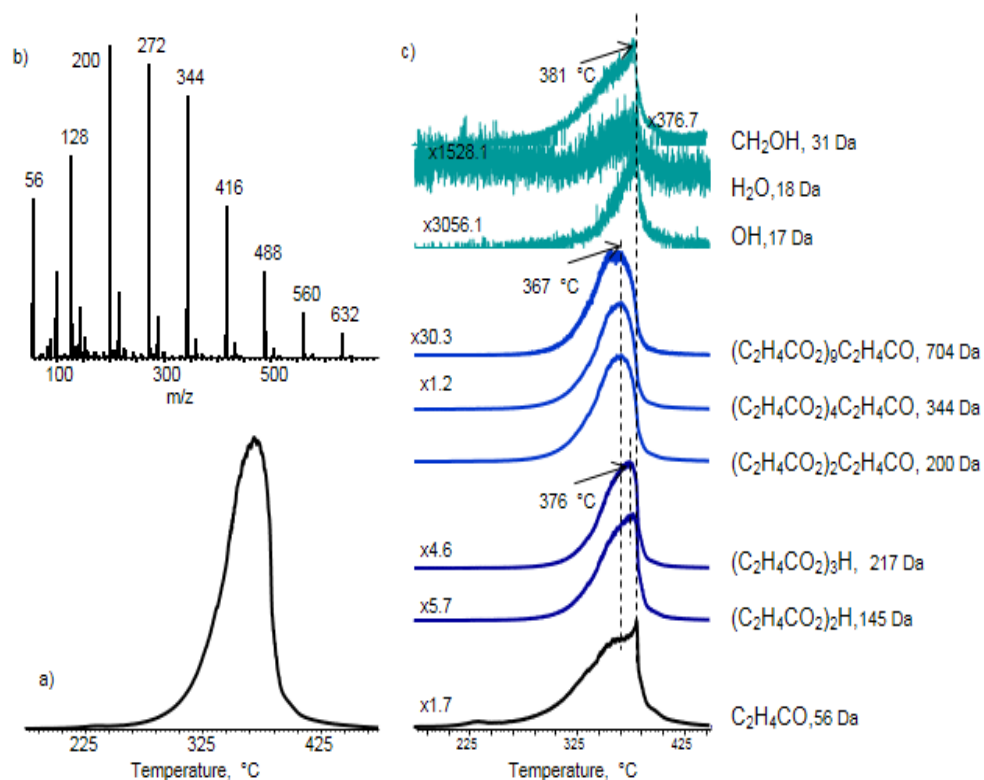
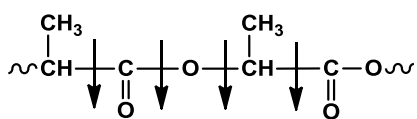
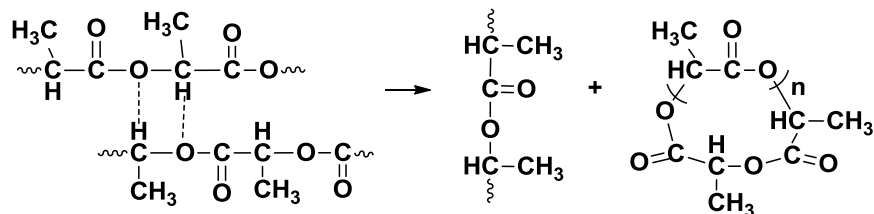


Figure 3.11. a) The TIC curve, b) the pyrolysis mass spectrum and c) the single ion evolution profiles of fragments recorded during the pyrolysis of PLA.

a) Random chain scissions

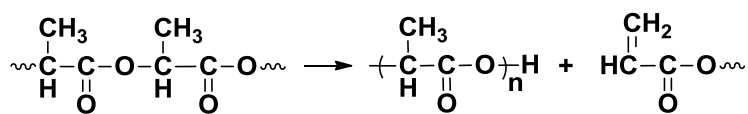


b) Trans-esterification reactions



Scheme 3.1. Thermal degradation of poly(lactic acid).

c) Cis-elimination reactions



Scheme 3.2. (Continued) Thermal degradation of poly(lactic acid).

Single ion evolution profiles of some of the representative fragments of PLA, such as C₂H₄CO (56 Da), (C₂H₄CO₂)₂H (145 Da), (C₂H₄CO₂)₃H (217 Da), (C₂H₄CO₂)₂C₂H₄CO (200 Da), and (C₂H₄CO₂)₄C₂H₄CO (344 Da) (C₂H₄CO₂)₉C₂H₄CO (704 Da) are shown in Figure 3.12.c. The trends in the single ion pyrograms reveal that the products generated by trans-esterification reactions are eliminated at slightly lower temperatures than those produced by random chain scissions and cis-elimination reactions. The evolution profiles of OH, H₂O and CH₂OH that may be generated during the pyrolysis of PLA composites are also included in the figure for comparison.

3.2.3.2. Cloisite 30B

The TIC curve of organically modified montmorillonite, Cloisite 30B and the pyrolysis mass spectra recorded at peak maxima are given in Figure 3.12. The base peak is at 296 Da that may be associated with both C₁₈H₃₇(CH₃)NCH₂, and/or CH₃N(C₁₆H₃₀)C₂H₄OH fragments, in the mass spectrum recorded at around 261°C. Other intense peaks can readily be attributed to C₃H₆NH₂ (58 Da), CH₃N(CH₂)C₂H₄OH (88 Da) and C₁₆H₃₃(CH₃)NCH₂, and/or CH₃N(C₁₄H₂₆)C₂H₄OH (268 Da) fragments in accordance with the classical fragmentation mechanisms of amines. The mass spectra recorded at elevated temperatures, at around 420°C, showed significantly different fragmentation pattern than those recorded at around 261°C that may be associated with decomposition of a high molecular weight hydrocarbon.

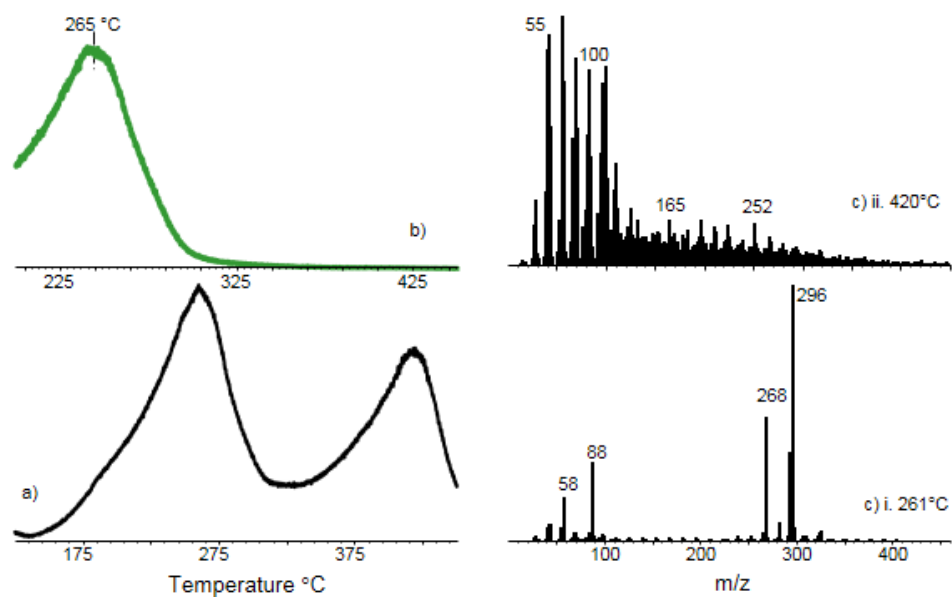


Figure 3.12. Pyrolysis mass spectrum of NC.

3.2.3.3. *BDBA*

The total ion current curve and the pyrolysis mass spectrum at the maximum of the TIC curve, at around 216°C, recorded during the pyrolysis of BDBA are shown in Figure 3.13. The mass spectrum is dominated by peaks at 45, 51, 78, 104, 130 and 166 Da that can be attributed to $B(OH)_2$, C_4H_5 , C_6H_6 , OBC_6H_5 , OBC_6H_4BO and molecular ions respectively. The spectrum is in accordance with the mass spectrum of BDBA given in NIST Mass Library indicating evaporation of BDBA at around 216°C under the high vacuum conditions of the mass spectrometer.

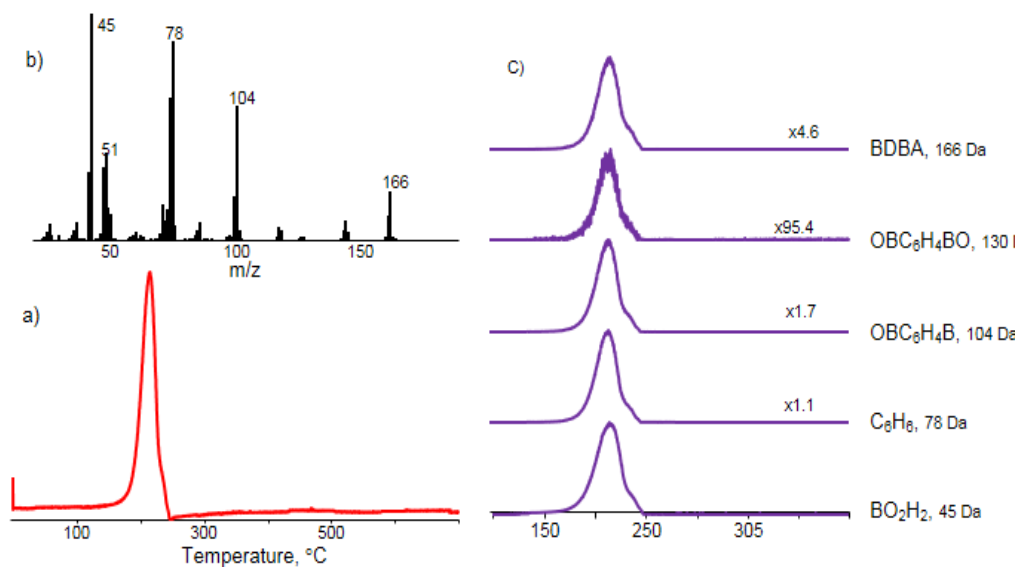


Figure 3.13. a) The TIC curve, b) the pyrolysis mass spectrum and c) the single ion evolution profiles of selected fragment recorded during the pyrolysis of BDBA.

3.2.3.4. PLA-ZnB

The total ion current curves, and the pyrolysis mass spectra at the maximum of the TIC curves, recorded during the pyrolysis of PLA composites involving 1, 2 or 3% ZnB are depicted in Figure 3.14. The corresponding data for pure PLA are also included for comparison. Significant decrease in thermal stability of PLA is noted upon addition of 1% ZnB. As the amount of ZnB incorporated is increased, a shoulder at elevated temperatures appeared in the TIC curve of the composites. The mass spectra recorded at TIC maxima indicate extensive fragmentation. However, the mass spectra recorded at around the high temperature shoulder indicate noticeable increase in the relative intensities of high mass fragments.

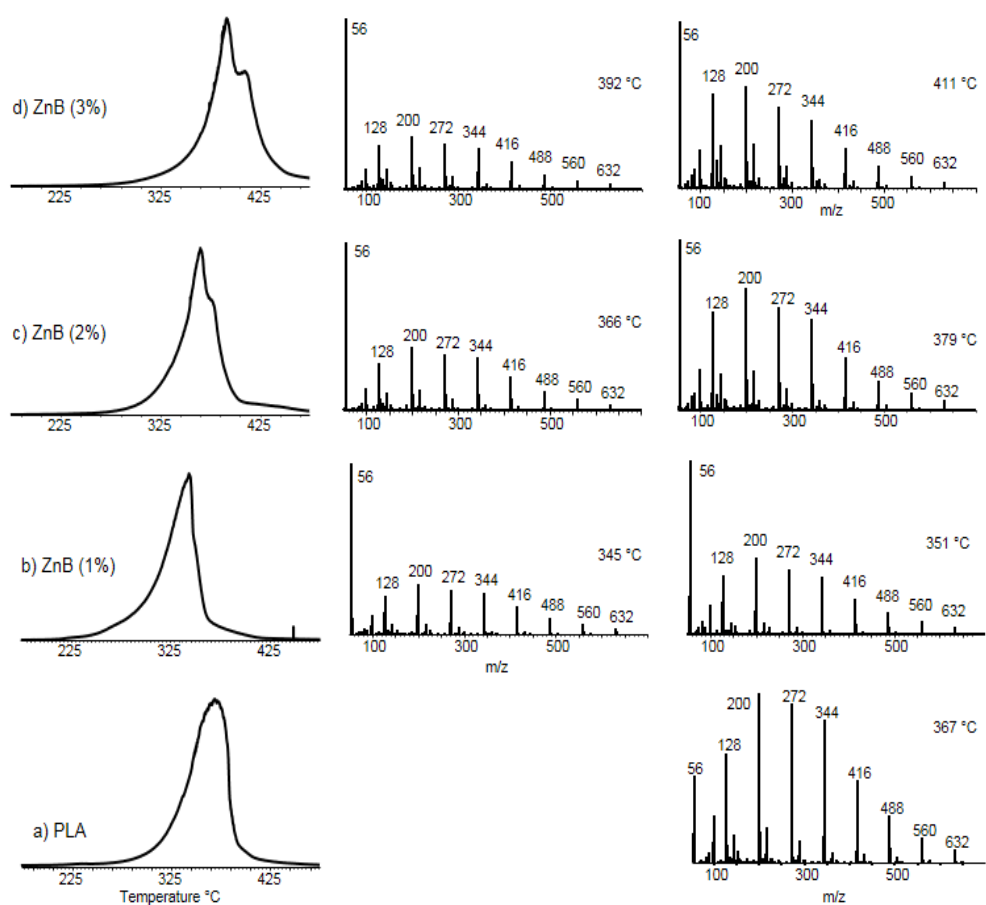


Figure 3.14. The TIC curves and the pyrolysis mass spectra of PLA and PLA composites involving 1, 2, and 3 % ZnB.

In Figure 3.15, the single ion evolution profiles of characteristic degradation products of PLA C_2H_4CO (56 Da), $(C_2H_4CO_2)_2H$ (145 Da), $(C_2H_4CO_2)_3H$ (217 Da), $(C_2H_4CO_2)_2C_2H_4CO$ (200 Da), and $(C_2H_4CO_2)_4C_2H_4CO$ (344 Da) are given. A careful study of the pyrolysis mass spectra and the evolution profiles of fragment ions indicate evolution of H_2O and 44 Da fragment at slightly lower temperatures. The fragment with m/z value 44 Da can directly be attributed to CO_2 . However, the evolution profile of CO_2 is almost similar with those of the low mass PLA based products as expected when generated during the pyrolysis of virgin PLA, on the other hand, it shows noticeable differences for the samples

involving ZnB. The relative yield of 44 Da fragment is increased as the amount of ZnB in the PLA composite increases. In addition, the maximum yields are reached at slightly lower temperatures. It may be thought that during the blending and/or pyrolysis process trans-esterification reactions between H₂O molecules present in the ZnB structure and PLA takes place which in turn lead to degradation of PLA chains as shown in Scheme 3.2. The pyrolysis mass spectra recorded at the maxima of the TIC curves indicate extensive fragmentation and decrease in the relative yields of both cyclic and protonated oligomers in accordance with this proposal. However, BO groups may also act as a crosslinking agent. Then, it can be concluded that BO₂H groups generated during these reactions contribute to the intensity of CO₂ peak at 44 Da fragment.

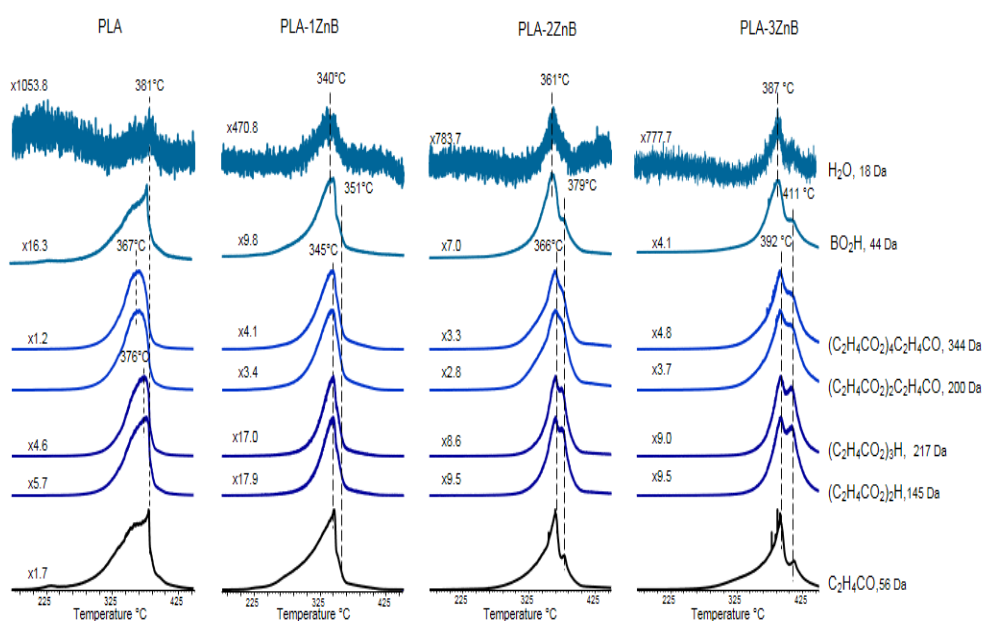
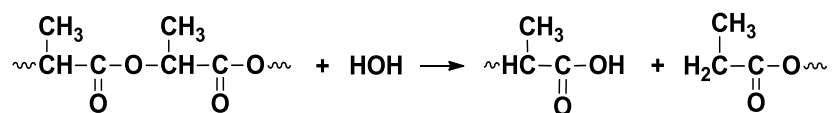


Figure 3.15. The single ion evolution profiles of selected fragment recorded during the pyrolysis of PLA and PLA composites involving 1, 2, and 3 % ZnB.



Scheme 3.3. Degradation of polylactide by hydrolysis reaction.

3.2.3.5. PLA-ZnB-NC

The total ion current curves and the pyrolysis mass spectra at the maximum of the TIC curves, recorded during the pyrolysis of PLA-C30B composites involving 1, 2 or 3 % ZnB are depicted in Figure 3.16. The related data for PLA-C30B is also included for comparison. It can be noted from the figure that upon incorporation of Cloisite 30B to PLA-ZnB composites, in general, the relative intensities of low mass fragments are increased. The TIC curves show also a peak or shoulder below 300°C, indicating that thermal degradation starts at relatively low temperatures. In addition, the high temperature peaks present in the TIC curves of PLA-ZnB composites involving 1 and 3% ZnB reaches maxima at slightly lower temperatures. In contrast, for the composite involving 2% ZnB the TIC curve shifts slightly to higher temperatures. But, even for this sample the relative yields of high mass fragments decrease compared to PLA composite involving only Cloisite 30B.

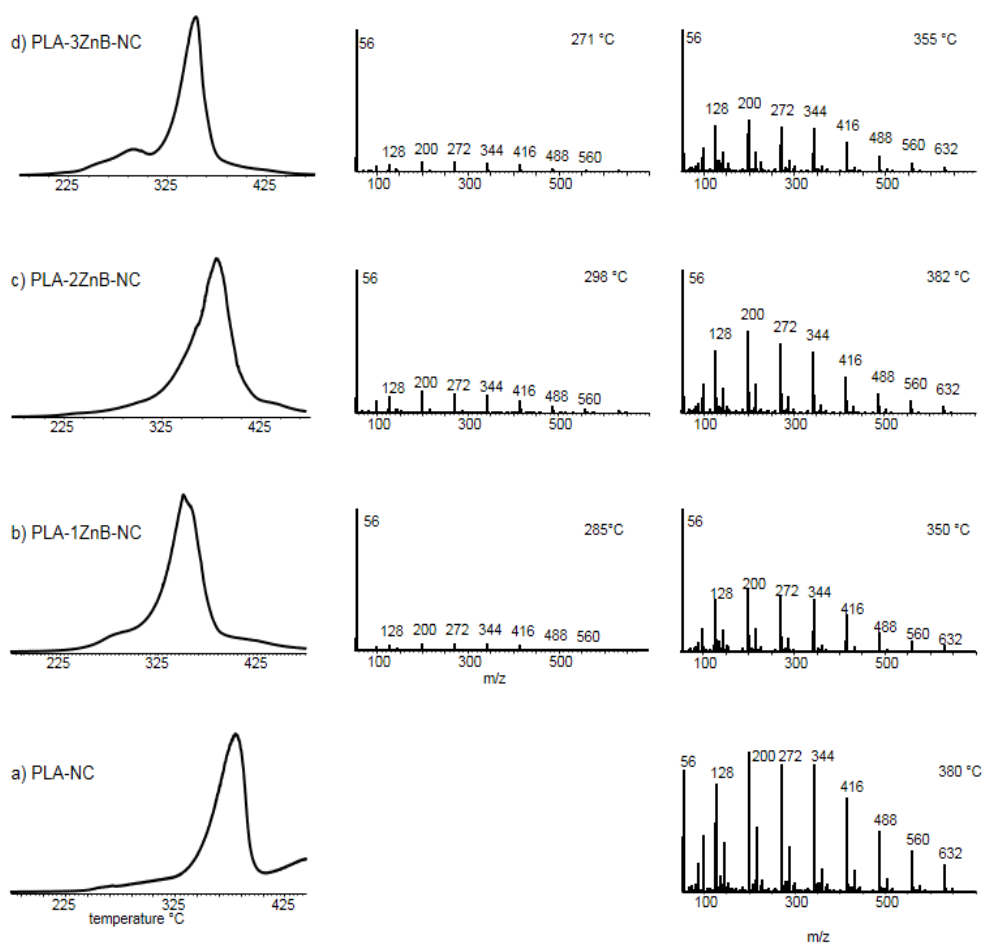


Figure 3.16. The TIC curves and the pyrolysis mass spectra of PLA-NC and PLA-NC composites involving 1, 2, and 3 % ZnB.

In Figure 3.17, the single ion evolution profiles of C_2H_4CO (56 Da), $(C_2H_4CO)_2H$ (145 Da), $(C_2H_4CO)_3H$ (217 Da), $(C_2H_4CO)_2C_2H_4CO$ (200 Da), $(C_2H_4CO)_4C_2H_4CO$ (344 Da) characteristic degradation products of PLA, $C_{18}H_{37}(CH_3)NCH_2$, and/or $CH_3N(C_{16}H_{30})C_2H_4O$ (296 Da) diagnostic fragment of Cloisite 30B, and BO_2H (44 Da) are given in Figure 3.17.

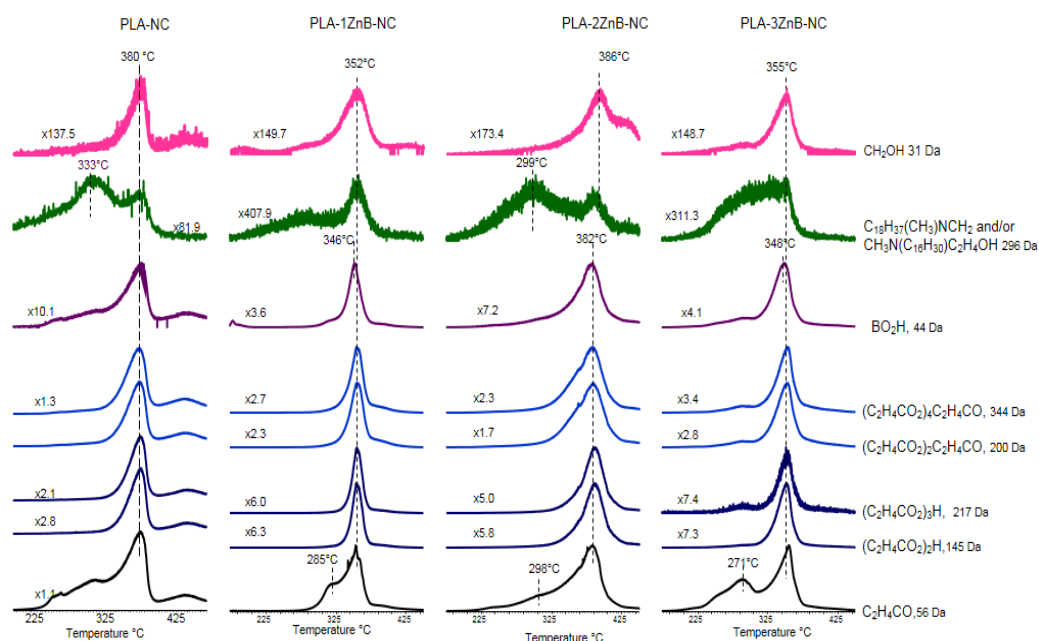
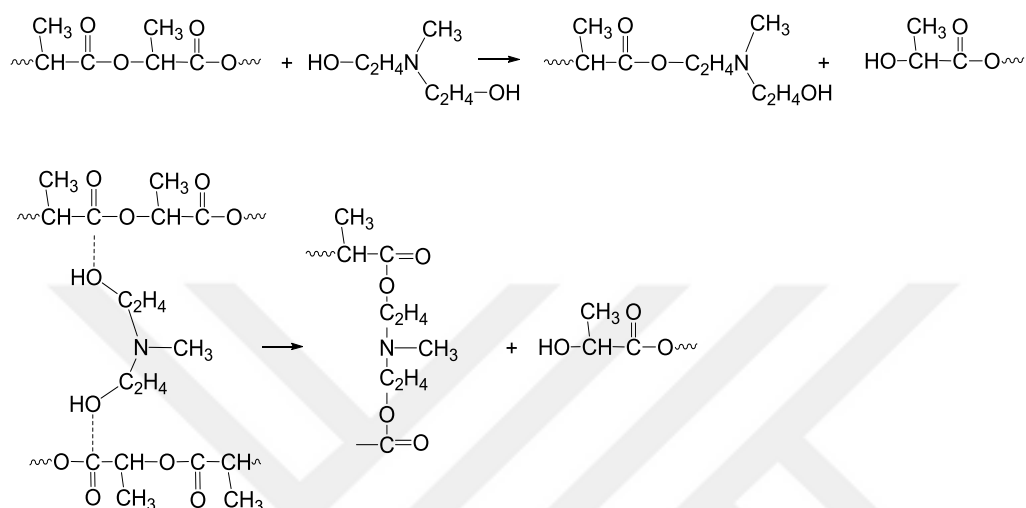


Figure 3.17. The single ion evolution profiles of selected fragment recorded during the pyrolysis of PLA-NC and PLA-NC composites involving 1, 2, and 3 % ZnB.

The evolution of 296 Da fragment occurs at elevated temperatures where thermal decomposition of PLA-ZnB composite takes place. In a recent study on PLA-C30B composites, strong evidences for interactions between the organic modifier of C30B and PLA, as shown in Scheme 3.3, was detected [81]. This trans-esterification reaction was supported by the increase in the relative yields of the products generated by cis-elimination reactions, the protonated oligomers, CH₂OH and OH fragments. The single ion evolution profiles of 296 Da fragment, the diagnostic product of C30B, generated during the pyrolysis of PLA-C30B composites involving ZnB show identical trends with that recorded during the pyrolysis of PLA-C30 indicating similar interactions with PLA chains. However, for the composites involving ZnB the relative yields of all high mass fragments including protonated oligomers are decreased. On the other hand, elimination of CH₂OH and OH groups at high temperatures are again

enhanced significantly. Thus, it may be concluded that interactions between the organic modifier of the montmorillonite and PLA take place also for the composites involving ZnB.



Scheme 3.4. Trans-esterification reactions between the organic modifier of Cloisite 30B and PLA.

On the other hand, it is clear that in general thermal stability of PLA-ZnB composites decreases upon incorporation of C30B, which is contrary to general expectations. Thus, it may be concluded that the delamination of silicate layers within the polymer chains, may cause a decrease in interaction between PLA and ZnB. Consequently, decrease in the extent of crosslinking may be expected. On the other hand, H₂O eliminated from ZnB may be trapped in C30B galleries which may increase the possibility of hydrolysis reactions causing the degradation of PLA chains at lower temperatures into small fragments. Actually, the slight increase in the thermal stability for the sample involving 2 % ZnB may be an indication of an optimum amount of ZnB for which the overall effect is

positive. However, in order to make a conclusion additional experiments have to be performed.

3.2.3.6. PLA-BDBA

The total ion current curves, and the pyrolysis mass spectra at the maximum of the TIC curves, recorded during the pyrolysis of PLA composites involving 1, 2 or 3% BDBA are depicted in Figure 3.18. The corresponding data for the pure PLA are also included in the figure for comparison.

The TIC curve of PLA composite involving 1% BDBA slightly shifts to low temperatures compared to virgin PLA. However, as the amount of BDBA added is increased thermal degradation of PLA occurs at higher temperatures indicating enhancement in thermal stability. The pyrolysis mass spectra of PLA-BDBA composites recorded at peak maxima are almost identical with the corresponding one of pure PLA except small differences in the relative abundances. On the other hand, the mass spectra recorded below 300°C are significantly different compared to those of virgin polymer. The relative intensities of peaks at 78, 104, 130, 158, 203, 230, and 274 Da are increased drastically. Presence of peaks at 78, 104 and 130 Da indicates elimination of BDBA fragments, C_6H_6 , OBC_6H_5 , and OBC_6H_4BO . On the other hand high mass peaks may be associated with fragments produced by decompositions of units generated by interactions of PLA with BDBA.

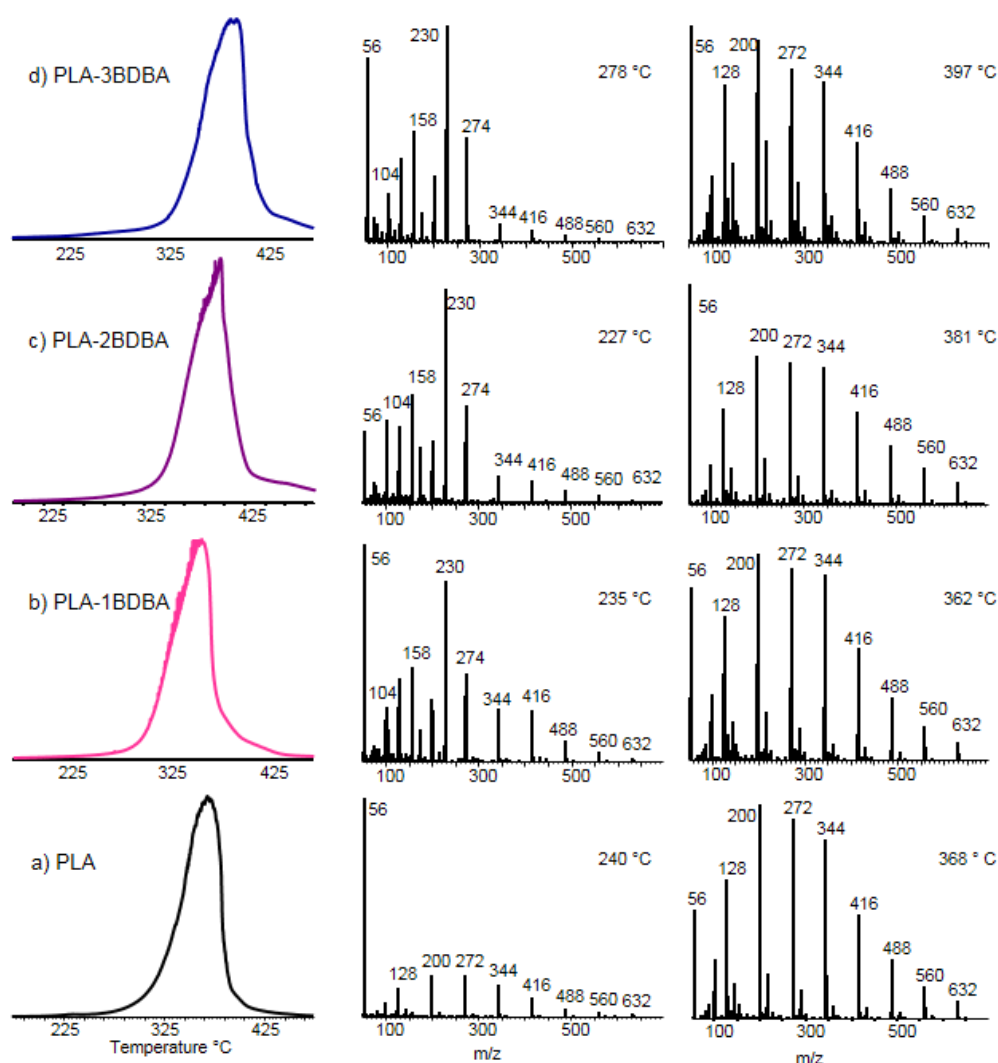


Figure 3.18. The TIC curves and the pyrolysis mass spectra of PLA and PLA composites involving 1, 2, and 3% BDBA.

In order to get a better insight single ion evolution profiles are examined and grouped according to the trends observed. Single ion evolution profiles of characteristic degradation products of PLA namely C_2H_4CO (56 Da), $(C_2H_4CO)_2H$ (145 Da), $(C_2H_4CO)_3H$ (217 Da), $(C_2H_4CO)_2C_2H_4CO$ (200 Da), and $(C_2H_4CO)_4C_2H_4CO$ (344 Da) are given in Figure 3.19. In addition, evolution profiles of fragments with m/z values 130, 203 and 230 Da showing

identical trends are included in the figure. It can be observed from the figure that the thermal degradation pathways of PLA involving trans-esterification reactions are suppressed as the amount of BDBA added to PLA matrix is increased. In contrast a slight increase in the relative yields of protonated oligomers is detected, however still products due to trans-esterification reactions are eliminated at slightly lower temperatures.

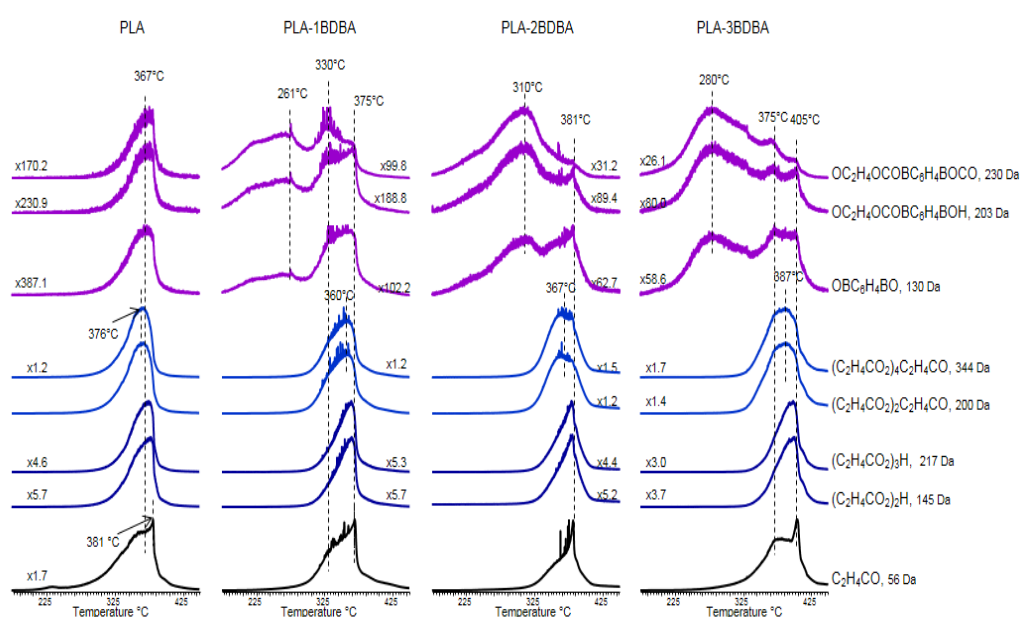
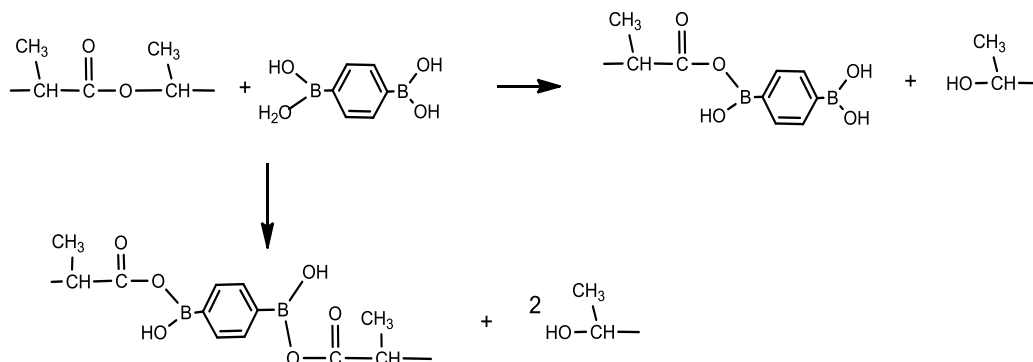


Figure 3.19. The single ion evolution profiles of selected fragment recorded during the pyrolysis of PLA and PLA composites involving 1, 2, and 3 % BDBA.

It may be thought that the OH groups of BDBA reacts with ester groups of PLA as shown in Scheme 3.4. Then the peaks at 203, 230 and 274 Da may be associated with $\text{OC}_2\text{H}_4\text{OCOBC}_6\text{H}_4\text{BOH}$, $\text{OC}_2\text{H}_4\text{OCOBC}_6\text{H}_4\text{BOCO}$ and $\text{OC}_2\text{H}_4\text{OCOBC}_6\text{H}_4\text{BOCOC}_2\text{H}_4\text{O}$ respectively. These trans-esterification reactions may cause degradation of PLA at slightly lower temperatures at least

to a certain extent. However, they may also generate a cross-linked structure leading an increase in thermal stability.



Scheme 3.5. Reaction between OH groups of BDBA with ester groups of PLA.

Some of these fragments are also observed during the pyrolysis of pure PLA due to fragments $\text{CHCO}_2(\text{C}_2\text{H}_4\text{CO}_2)\text{H}$, (130 Da), $\text{CH}_2\text{CO}_2(\text{C}_2\text{H}_4\text{CO}_2)_2\text{H}$ (203 Da), $(\text{C}_2\text{H}_4\text{CO}_2)_3\text{CH}_2$, (230 Da) and $\text{CO}_2(\text{C}_2\text{H}_4\text{CO}_2)_3\text{CH}_2$ (274 Da) that may be generated during thermal and/or dissociative ionization processes. However, their evolution profiles are identical with those of the characteristic thermal degradation products of PLA. In addition their relative yields are increased with the increase in amount of BDBA supporting the proposed mechanism. The low temperature eliminations may be associated with BDBA units present as chain end groups. However, as the losses of these fragments are also enhanced in the temperature region where PLA decomposition takes place, it may be thought that as the extent of crosslinking increases the units involving boron linkages decompose at elevated temperatures where PLA degradation occurs.

3.2.3.7. PLA-BDBA-NC

The total ion current curves and the pyrolysis mass spectra at the maximum of the TIC curves, recorded during the pyrolysis of PLA-NC composites involving

1, 2 or 3% BDBA are shown in Figure 3.20. The corresponding data for the pure PLA are also included in the figure for comparison. The TIC curve of neat PLA-NC shifts slightly to low temperature regions upon addition of 1% BDBA. Further addition of BDBA causes increase in thermal stability as in case of pristine PLA.

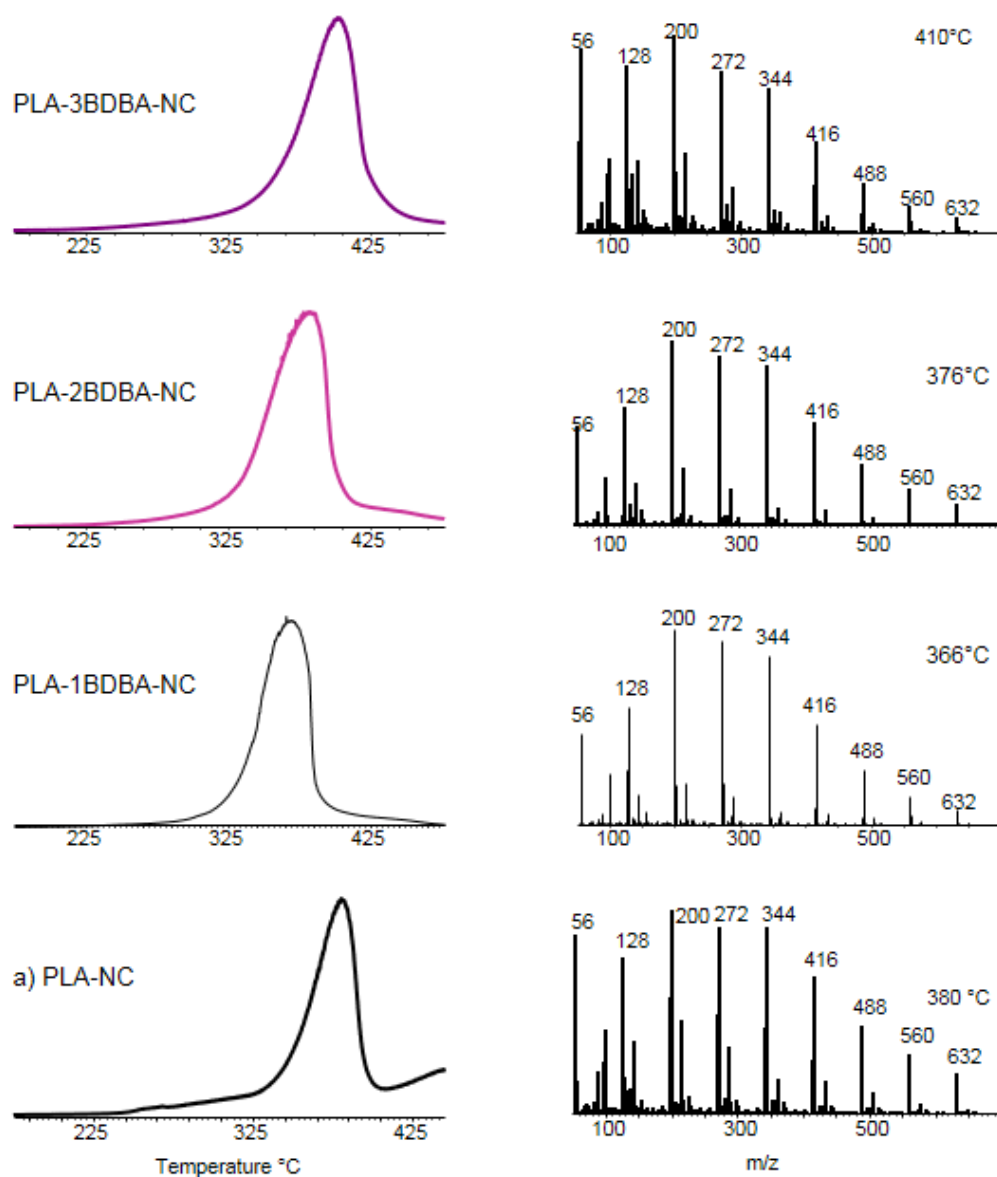


Figure 3.20. The TIC curves and the pyrolysis mass spectra of PLA-NC and PLA-NC composites involving 1, 2, and 3% BDBA.

Single ion evolution profiles of characteristic degradation products of PLA C_2H_4CO (56 Da), $(C_2H_4CO)_2H$ (145 Da), $(C_2H_4CO)_3H$ (217 Da), $(C_2H_4CO)_2C_2H_4CO$ (200 Da), and $(C_2H_4CO)_4C_2H_4CO$ (344 Da) and those related to fragments generated due to reactions between PLA and BDBA namely $CHCO_2(C_2H_4CO)_2H$ (130 Da), $CH_2CO_2(C_2H_4CO)_2H$ (203 Da), $(C_2H_4CO)_3CH_2$, (230 Da) and diagnostic fragment of Cloisite 30B, both $C_{18}H_{37}(CH_3)NCH_2$, and/or $CH_3N(C_{16}H_{30})C_2H_4O$ (296 Da) are given in Figure 3.21. The PLA based products show identical evolution profiles and increase in relative yields of protonated oligomers are detected as in case of PLA-C30B.

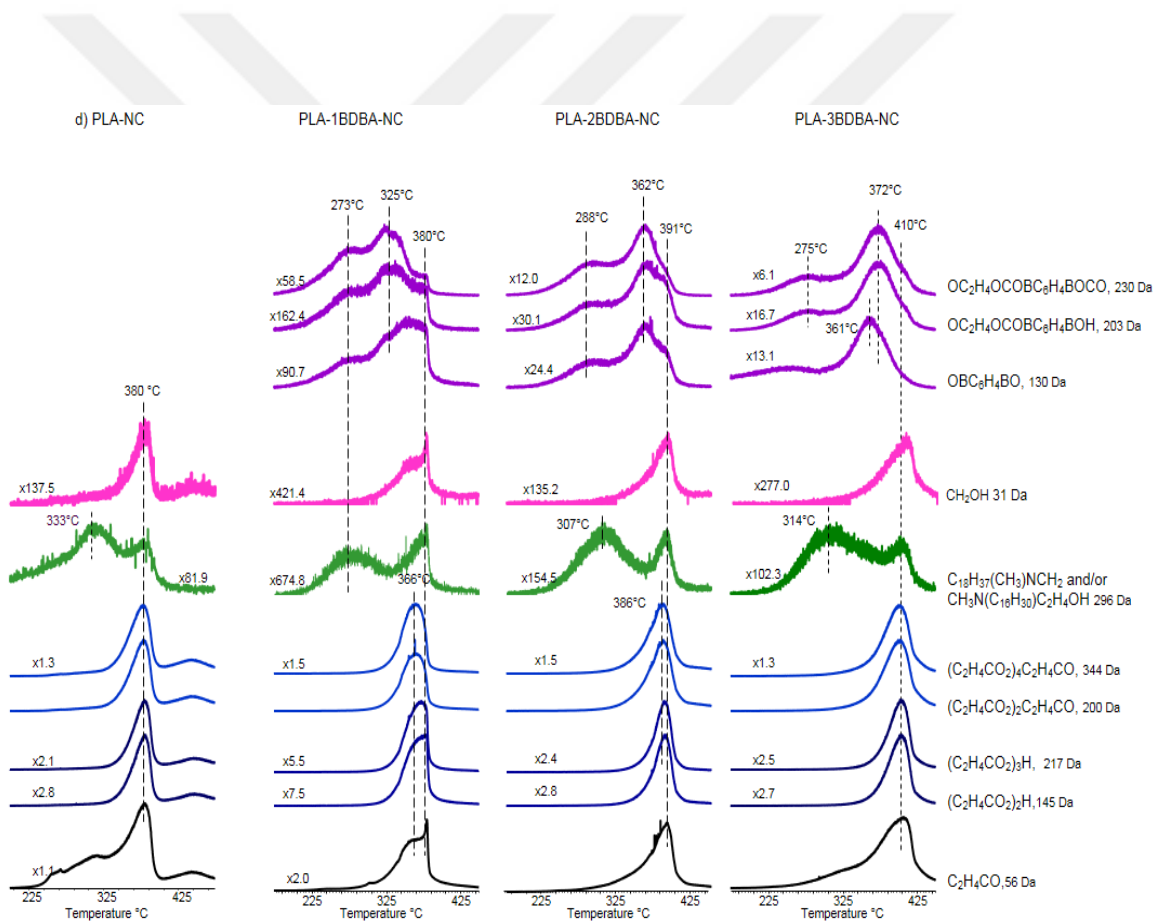


Figure 3.21. The single ion evolution profiles of selected fragment recorded during the pyrolysis of PLA-NC and PLA-NC composites involving 1, 2, and 3 % BDBA.

Relative yields of products generated as a consequence of reactions between PLA and BDBA are increased noticeably in the presence of nanoclay. Loss of these products is observed mainly at elevated temperatures. Thus, it can be concluded that the interactions of boron compound with PLA are enhanced when the molecules are trapped in clay galleries.

3.3. Mechanical Properties

3.3.1. Tensile Test

The effect of type and composition of additives and reinforcement material on mechanical properties of PLA were investigated for melt compounded NCs by the measurement of the universal tensile testing according to ASTM D638 standards. In Table 3.3, the tensile strength, percentage strain and Young's modulus values for PLA, PLA with boron additives and PLA-boron compounds-organoclay composites are tabulated. Tensile measurements of each nanocomposites were carried out at least five times and the average values are given in the table. Standard deviations of each measurement are also stated.

Table 3.3. Tensile strength, percentage strain and Young's modulus properties for PLA, PLA with boron additives and PLA-boron compounds-organoclay composites.

SAMPLES	Tensile Strength (MPa)	Elongation at break (%)	Young's modulus (GPa)
PLA	64.5 ± 1.30	11.0 ± 0.50	1.18 ± 0.03
PLA-1ZnB	64.2 ± 2.15	9.5 ± 0.50	1.18 ± 0.03
PLA-2ZnB	65.6 ± 1.70	8.6 ± 0.30	1.31 ± 0.04
PLA-3ZnB	63.2 ± 2.00	8.4 ± 0.50	1.21 ± 0.04
PLA-1ZnB-NC	69.4 ± 1.62	10.1 ± 0.45	1.26 ± 0.03
PLA-2ZnB-NC	69.2 ± 1,31	8.44 ± 0.48	1.26 ± 0.02
PLA-3ZnB-NC	65.2 ± 1.74	8.85 ± 0.11	1.35 ± 0.02
PLA-1BDDA	69.3 ± 1.12	9.2 ± 0.52	1.27 ± 0.05
PLA-2BDBA	60.5 ± 1.20	9.1 ± 0.45	1.24 ± 0.03
PLA-3BDBA	51.5 ± 1.30	8.2 ± 0.50	1.26 ± 0.04
PLA-1BDBA-NC	65.4 ± 1.17	8.7 ± 0.23	1.26 ± 0.03
PLA-2BDBA-NC	54.9 ± 1.95	7.7 ± 0.30	1.24 ± 0.03
PLA-3BDBA-NC	51.2 ± 0.80	7.2 ± 0.03	1.27 ± 0.02

In Figure 3.22, the tensile strengths of neat PLA and PLA with additive(s) are projected from the data above. As observed from Figure 3.23, change in tensile strength was not significant with the addition of zinc borate (ZnB) with respect to neat PLA. When the composition of ZnB is increased, the effect of this compound on tensile strength may be neglected considering the change of tensile

strength values were within the range of the error margin. Further increase in ZnB content showed no significant change in tensile properties of PLA. However, addition of nanoclay to PLA-ZnB composite increased the tensile strength of the resultant material considerably, except PLA-3ZnB-NC.

As given in tensile strength data presented below; the addition of 1% BDBA into neat PLA increased the tensile strength. As the amount of BDBA was increased, the decrease in tensile strength becomes more obvious which could be attributed to the adverse effect on PLA matrix. Furthermore, the addition of 3% C30B into PLA-BDBA composite resulted in even lower tensile strength values and the lowest tensile strength was measured for PLA-3BDBA-NC sample. This situation can be given as a good example of antagonistic effect.

As seen in SEM images in Figure 3.1 and 3.2, formation of agglomeration can be observed for 3% ZnB containing composite, and for BDBA addition; agglomerations begins at 2% loading level and become obvious for 3% containing composite. These agglomerates causes the reduction of mechanical properties of composites which is in accordance with tensile test results.

The best results were obtained for 1% and 2% ZnB containing composites and the lowest loading level (1%) of BDBA with organoclay addition.

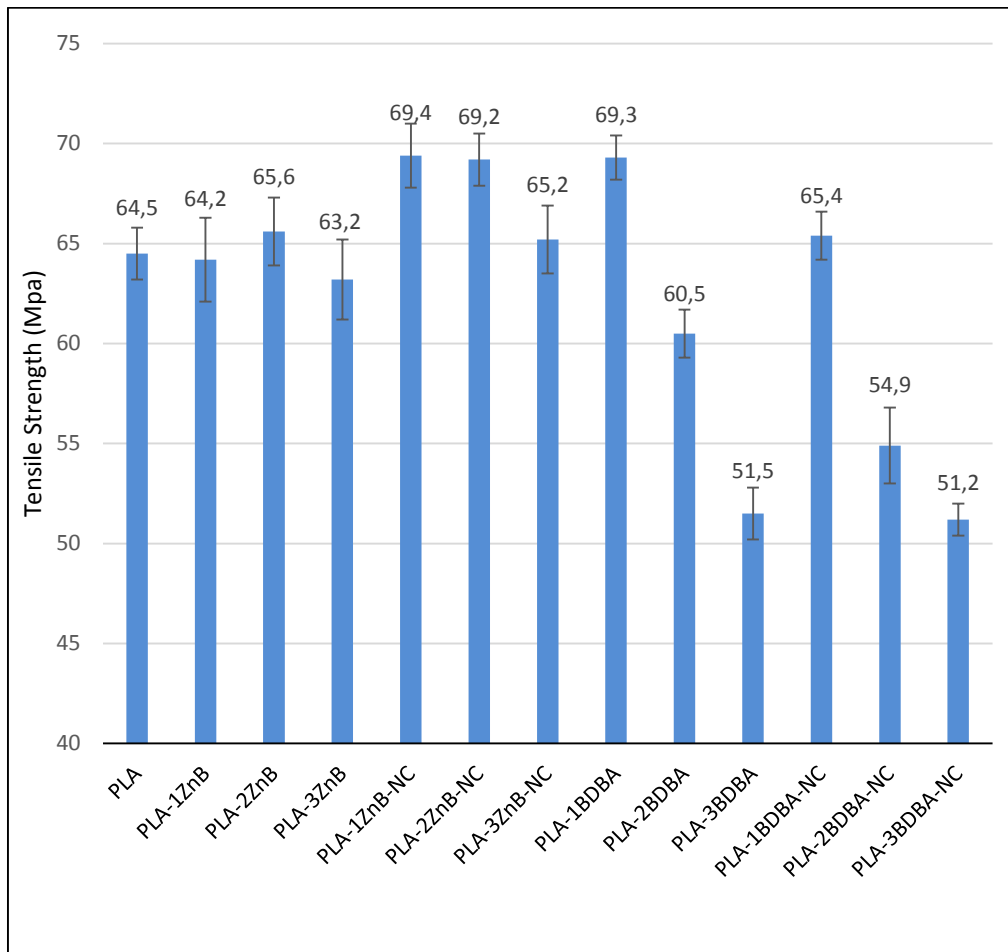


Figure 3.22. Tensile strengths of PLA, PLA with boron additives and PLA-boron compounds-organoclay nanocomposites.

In Figure 3.23, the percentage elongation of neat PLA and PLA with additive(s) are projected. As seen in the projection below, addition of ZnB into neat PLA decreases the percentage elongation gradually, which means the percent strain at break is decreased and corresponding ultimate strengths for these samples are lowered. This may be due to the lack of stress transfer between ZnB particles and PLA chains. On the other hand, addition of organoclay into PLA-ZnB composite somewhat increases the percentage elongation (except for the case of 2% ZnB addition). The addition of clay as rigid filler is expected to decrease the ultimate elongation.

In the case of addition of BDBA; the decrease in percentage elongation of material is more prominent compared to ZnB addition. But, in contrast to PLA-ZnB-NC composite; the addition of nanoclay into PLA-BDBA composite further decreases the elongation percentage.

Actually, the changes in elongation values may not be accepted as considerable except for PLA-2BDBA-NC and PLA-3BDBA-NC, which exhibits the lowest elongation results among all the prepared composites.

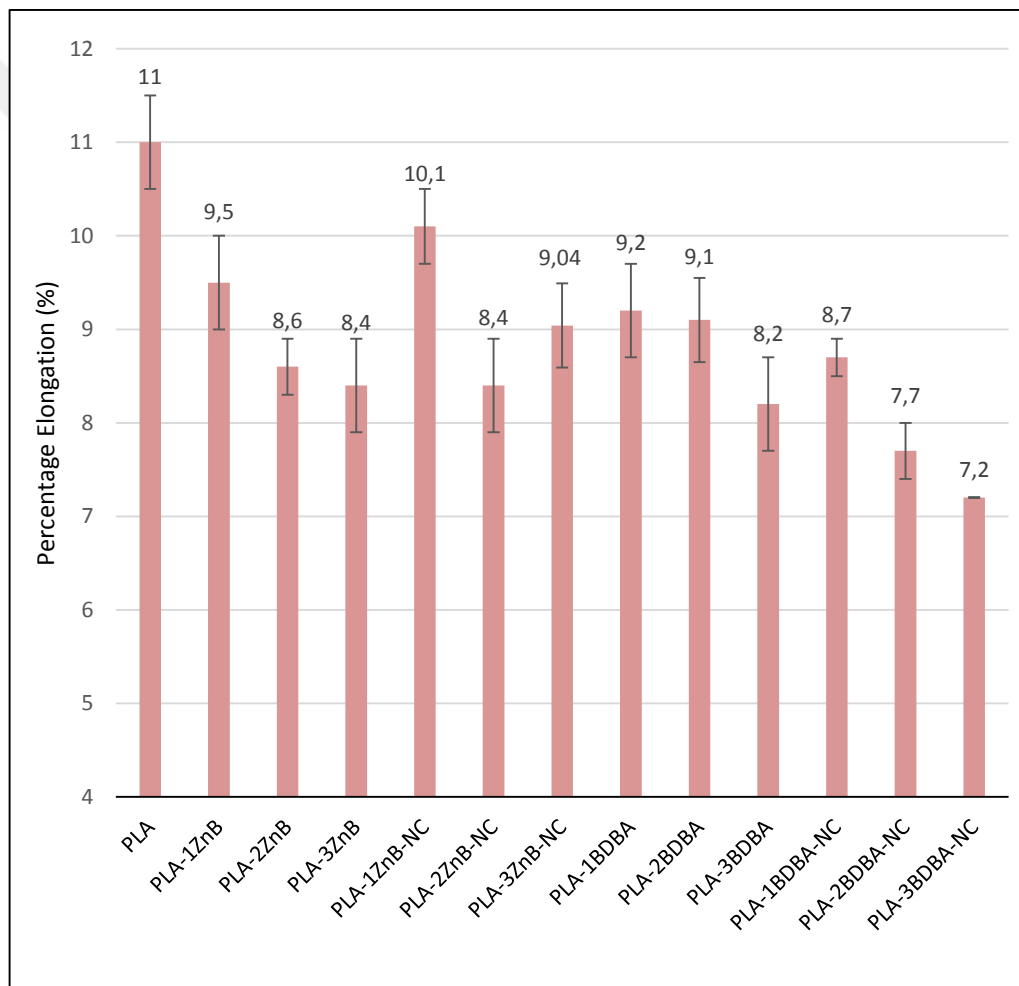


Figure 3.23. Percentage elongation of PLA, PLA with boron additives and PLA/boron compounds/organo clay nanocomposites.

In Figure 3.24, Young's modulus of neat PLA and PLA with additive(s) are projected. As given in Figure 3.24, a slight increase in Young's modulus is recorded for all PLA-boron additive-clay composites. Addition of organoclay usually increases the modulus for all composites. The addition of boron compounds into PLA slightly increases the modulus. The increase is more significant for BDBA. For PLA-2ZnB and PLA-3ZnB-NC cases; the data gathered are significantly higher than other values. In general, addition of solid increase the Young's modulus, but the results are found as almost the same.

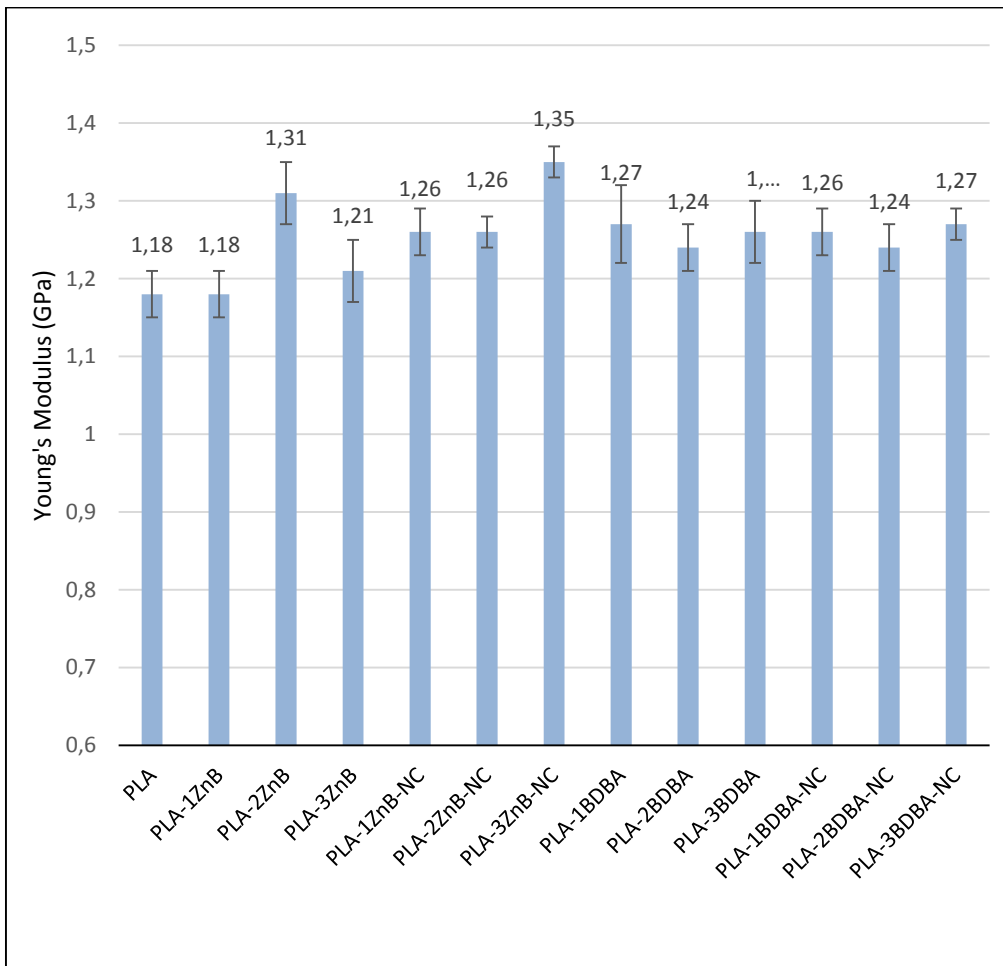


Figure 3.24. Young's modulus of neat PLA, PLA with boron additives and PLA/boron compounds/organoclay nanocomposites.

3.4. Flammability Properties

3.4.1. UL-94 Ratings

The UL-94 ratings and observation made for PLA composites prepared are summarized in Table 3.4.

Table 3.4. UL-94 ratings and observations during UL-94 test for the samples prepared.

SAMPLES	UL-94	Observations
PLA	NR	Afterflame plus afterglow time is greater than 30 s, cotton indicator ignited by drops.
PLA-1ZnB	NR	Burned slower than neat PLA.
PLA-2ZnB	NR	Burned slightly slower than PLA-1ZnB.
PLA-3ZnB	NR	Burning propagation is slower than PLA-2ZnB.
PLA-1ZnB-NC	NR	Slightly char formation on the edge of sample.
PLA-2ZnB-NC	NR	Slightly char formation is observed.
PLA-3ZnB-NC	NR	Char formation is observed and burning propagation is decreased while ZnB concentration is increased.
PLA-1BDDA	NR	Char formation, decrease in burning propagation compared to ZnB containing composites.
PLA-2BDBA	NR	Char formation.
PLA-3BDBA	NR	Char formation.

Table 3.5. (Continued) UL-94 ratings and observations during UL-94 test for the samples prepared.

PLA-1BDBA-NC	NR	Increase in char formation, burning propagation became slower than samples containing only BDBA.
PLA-2BDBA-NC	NR	Increase in char formation and reduction in burning propagation.
PLA-3BDBA-NC	NR	Increase in char formation and lowest burning propagation is observed.

NR: Not readed.

According to UL-94 vertical test standard, as listed in Table 3.4, ratings were obtained for neat PLA and related composites. Especially, inclusion of C30B affects char formation and causes a decrease in the burning propagation of the composites as a result. While ZnB slows down the burning propagation slightly, BDBA lowers the burning propagation significantly, as required. The slowest burning propagation is observed for PLA-3BDBA-NC.

After UL-94 tests, total burning time of all samples are found as more than 30 seconds (Table 3.4), but not possible to make classification according to UL-94 vertical test standard for those samples.

3.4.2. LOI Ratings

LOI and UL-94 tests were made to investigate the flame retardancy behavior of PLA composites. As seen from Figure 3.25, LOI value is slightly increased from 19.0 % to 19.8% with the addition of ZnB and nanoclay into PLA matrix. The inclusion of nanoclay with ZnB rises LOI values of PLA-ZnB with a factor of

0.3 at all concentrations by the help of synergistic effect of Cloisite 30B. The inclusion of BDBA results with increase at the lowest loading level (1%), further addition of BDBA exhibits decreasing trend of the LOI values of PLA composites. As mentioned earlier in SEM results (see Figure 3.2), the decrease in dispersion homogeneity is observed in composites that contain higher amount of BDBA and this causes reduction of flame resistance property. This is the general trend observed in Figure 3.25. Addition of nanoclay together with BDBA improves LOI values compared to composites containing only BDBA.

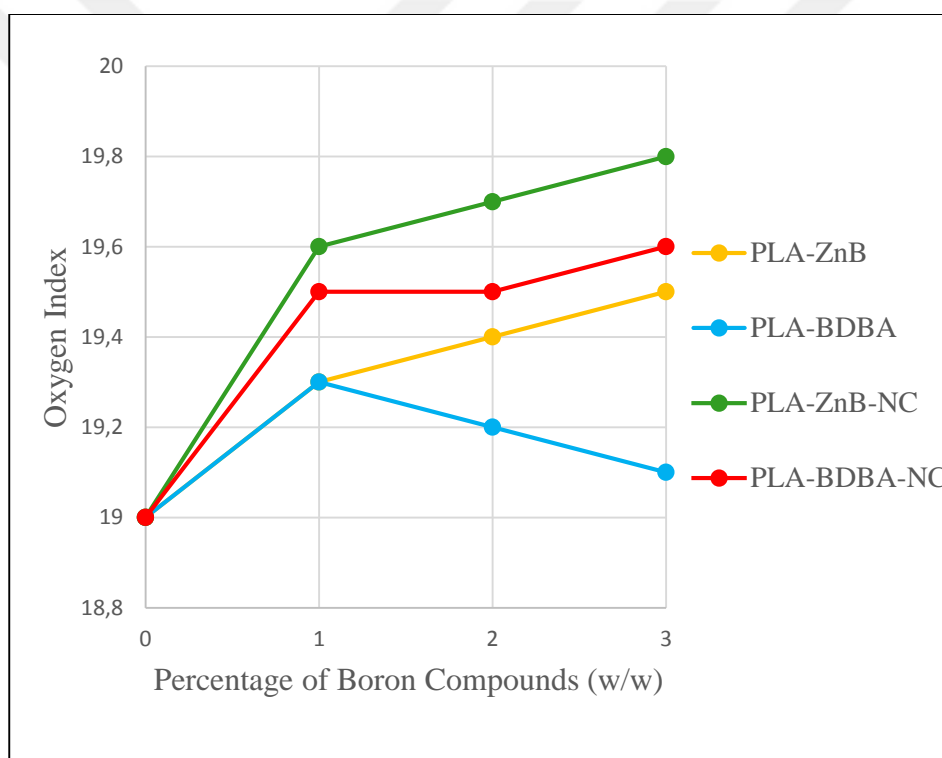


Figure 3.25. The LOI values of composites.



CHAPTER 4

CONCLUSIONS

In this study, zinc borate, ZnB, benzene-1,4-diboronic acid, BDBA and organically modified montmorillonite, Cloisite 30B, C30B containing nanocomposites of polylactide, PLA were prepared by melt mixing method. Effects of type and amount of boron compounds and nanoclay on mechanical, morphological, thermal and flammability properties of PLA based composites were investigated.

In order to analyze the morphology of the nanocomposites, SEM, TEM and XRD analyses were performed. SEM images of ZnB and BDBA containing composites revealed homogeneous dispersion for composites involving low concentration of boron compounds and agglomerations for high concentration of boron compounds. TEM images of PLA nanocomposites indicated presence of intercalated and exfoliated regions. The Bragg's peak of organically modified montmorillonite was disappeared in the XRD diffractograms of PLA nanocomposites involving 1, 2, 3 wt. % of boron compounds and 3 wt. % nanoclay in accordance with TEM results.

As ZnB is an inorganic compound, the composites with ZnB additives had a higher char yield compared to BDBA composites. This result confirmed the similarity (conformity) between the flame retardancy and thermal stability characteristics of the PLA-ZnB-NC composites.

DSC results indicated that incorporation of ZnB and BDBA did not affected glass transition temperature of PLA. On the other hand, melting temperatures of

the composites were observed at higher temperatures whereas cold crystallization temperatures were shifted to lower values compared to blank PLA. The increase in melting temperatures may be associated with more ordered crystal structures.

TGA results revealed slight increases in the char yields upon addition of boron compounds. Increase in decomposition rates and char yields was observed for C30B containing nanocomposites at the highest concentration of ZnB and BDBA. Decrease in decomposition temperature of PLA is more significant for ZnB containing composites.

DP-MS analyses indicated that the relative yields of products generated by transesterification and cis-elimination reactions were significantly enhanced during the pyrolysis of PLA composites compared to blank PLA. The increase in the relative yields of products generated by cis-elimination reactions were more pronounced for the composites also involving C30B. This behavior was associated with interaction between hydroxyl groups of the organic modifier of C30B and PLA. DPMS results also indicated that a decrease in thermal stability upon addition of 1% ZnB or BDBA. However, as the amount of boron compounds was increased thermal stability was increased. This behavior was associated with transesterification reactions between the boron compounds and PLA. These reactions, although caused decomposition of PLA chains at low concentrations of boron to a certain extent, generated a cross-linked structure increasing thermal stability. Incorporation of C30B into PLA composites involving 1 or 3% ZnB caused a decrease in thermal stability. An opposite trend is observed for the composite involving 2% ZnB. On the other hand, with the addition of C30B into for PLA composites involving BDBA, increase in thermal stability was detected. It may be concluded that the efficiency of crosslinking of ZnB was suppressed as a consequence of intercalated structures, while those of BDBA, being a small molecule that can diffuse into clay layer, were enhanced. To our surprise, there exist a significant temperature differences between TGA

and DPMS results. One possibility is the further mixing of the samples in chloroform solutions before DPMS analysis.

In terms of enhancement of tensile strength, 1 and 2 wt. % of BDBA gave the best results among composites containing boron compounds. However, PLA-ZnB nanocomposites showed higher tensile strength results after addition of nanoclay compared to PLA-BDBA nanocomposites involving nanoclay. Inclusion of boron compounds caused a very slight reduction in percent elongation of PLA. Nanoclay addition to ZnB filled composites showed an increase in elongation, whereas percent elongation decreased with the inclusion of nanoclay into PLA-BDBA composites. In the case of Young's modulus, additions of boron compounds and nanoclay caused slight improvement.

LOI value of PLA increased linearly as the amount of ZnB is increased. Nanoclay addition exhibited slight improvement in LOI both for ZnB or BDBA containing composites. Even low amounts of boron additive (1, 2 and 3 %) affected the flame retardancy of the resultant material, but the amount of improvement was insignificant.



REFERENCES

- [1] Fried, J. R. (2014) Introduction to Polymer Science. Polymer Science and Technology, 3rd Edition.
- [2] Kutz, M. (2011) Applied Plastics Engineering Handbook: Processing and Materials. Elsevier Science Publication. ISBN 978-1-437-73515-4.
- [3] Roberts, J. D., Caserio, M. C. (1977) Basic Principles of Organic Chemistry, Second Edition. W. A. Benjamin, Inc., Menlo Park, CA. ISBN 0-8053-8329-8.
- [4] Andrady, A. L., Neal, M. A. “Applications and Societal Benefits of Plastics”, *Philosophical Transactions of the Royal Society B*, **2009**; 364, 1977–1984.
- [5] Rydz J, Sikorska W, Kyulavska M, Christova D. “Polyester-Based (Bio) degradable Polymers as Environmentally Friendly Materials for Sustainable Development”, *International Journal of Molecular Sciences*, **2015**; 16, 564-596.
- [6] Al-Mulla, E. A. J., Ibrahim, N. A. “Poly (Lactic Acid) as a Biopolymer-Based Nano-Composite”. Products and Applications of Biopolymers: Part II”, *Intech Edition*, **2012**; 27-40.

- [7] Painter, P. C., Coleman, M. M. (2008) Essentials of Polymer Science and Engineering. DEStech Publications, Incorporated. ISBN 978-1-932-07875-6.
- [8] Ebewele, R. O. Chapter 1: Introduction. Polymer Science and Technology, 1st Edition. ISBN: 978-0-8493-8939-9.
- [9] Ray, S. S.; Okamoto, M. "Polymer/layered silicate nanocomposites: a review from preparation to processing". *Progress in Polymer Science*, **2003**; 28, 1539–1641.
- [10] Ghanbarzadeh B.; Almasi H. (2013) Biodegradable Polymers, Intech, <http://dx.doi.org/10.5772/56230>
- [11] Saldivar-Guerra, E.; Vivaldo-Lima, E. (2013) Handbook of polymer synthesis, characterization and processing. John Wiley & Sons, Inc., Publication. ISBN 978-0-470-63032-7.
- [12] Vroman, I., Tighzert, L. "Biodegradable Polymers". *Materials*, **2009**; 2, 307-344.
- [13] Navrátilová, N., Náplava, A. "Study of biodegradable plastics produced by injection molding", *Materials Science and Technology*, **2011**; 11, 48-53.
- [14] Casper, R. A., Dunn, R. L. "Method of producing biodegradable prosthesis and products", Google Patents.

url= <http://www.google.com.tr/patents/EP0146398A3?cl=en> [Last Accessed on September, 2015]

- [15] Kumar, A.; Gupta, R. K. (2003) Fundamentals of Polymer Engineering, Second Edition. Marcel Dekker, Inc. Basel, New York. ISBN: 0-8247-0867-9
- [16] Román, J. S., Aguilar, M. R. (2014) Smart Polymers and their Applications. Elsevier Science Publication. ISBN 978-0-857-09702-6.
- [17] Bhandari, B. (2012) Food Materials Science and Engineering. Wiley Publications. ISBN 978-1-118-37392-7.
- [18] Gruber, P.; O'Brien, M. Polylactides "Natureworks™ PLA". In Biopolymers: Polyesters III—Applications and Commercial Products; Steinbüchel, A., Doi, Y., Eds.; Wiley-VCH: Weinheim, Germany, **2002**; Volume 4, 235–239.
- [19] Ray, S. S.; Okamoto, M. "Polymer/layered silicate nanocomposites: a review from preparation to processing". *Progress in Polymer Science*, **2003**; 28, 1539–1641.
- [20] Weber, C. J., Haugaard, V., Festersen, R., Bertelsen, G. "Production and applications of biobased packaging materials for the food industry". *Food Additives and Contaminants*, **2002**; 19, 172-177.
- [21] Robertson, G. L. (2005) Food Packaging: Principles and Practice, Second Edition. Taylor & Francis. ISBN 978-0-849-33775-8.

- [22] Eissa-Mohamed, A. M. (2011) Synthesis and Characterization of Novel Biopolymers via Click Chemistry, Durham theses, Durham University. url= <http://etheses.dur.ac.uk/581/> [Last Accessed on September, 2015]
- [23] Rasal, R. M.; Janorkar, A. V.; Hirt, D. E. “Poly (lactic acid) modifications”. *Progress in Polymer Science*, **2010**; 35, 338–356.
- [24] Niaounakis, M. (2014) Biopolymers: Processing and Products. Elsevier Science. ISBN 978-0-323-27938-3.
- [25] Mohapatra, A. K.; Mohanty S.; Nayak S.K. “Dynamic mechanical and thermal properties of polylactide-layered silicate nanocomposites”. *Journal of Thermoplastic Composite Materials*, **2014**; 27, 699–716.
- [26] Mitrus, M.; Wojtowicz, A.; Moscicki, L. (2009) Thermoplastic Starch: Biodegradable Polymers and Their Practical Utility. Wiley-Vch Verlag GmbH & Co. ISBN: 978-3-527-32528-3.
- [27] Nicolae C. A., Grigorescu M. A., Gabor R. A. “An Investigation of Thermal Degradation of Poly (Lactic Acid)”. *Engineering Letter*, **2008**; 16, 568-604.
- [28] Signori, F.; Coltelli, M.B.; Bronco, S. “Thermal degradation of poly (lactic acid) (PLA) and poly (butylene adipate-co-terephthalate) (PBAT) and their blends upon melt processing”. In *Polymer Degradation and Stability*, **2009**; 94, 74–82.

- [29] Najafi N., Heuzey M. C., Carreau P. J., Wood-Adams P. M., “Control of thermal degradation of polylactide (PLA)-clay nanocomposites using chain extenders”, **2012**; 97, 554–565.
- [30] Ren, J. (2011) *Biodegradable Poly (Lactic Acid): Synthesis, Modification, Processing and Applications*. Springer-Verlag. ISBN 978-3-642-17596-1.
- [31] Akita, H., Hattori, T. *Journal of Polymer Science B: Polymer Physics*, *Journal of Polymer Science*, **1999**; 37, 189.
- [32] Montaudo, G. and Lattimer, R. P. (2012) *Mass Spectrometry of Polymers*, CRC Press, Boca Raton London New York Washington, D.C. ISBN 0-849-33127-7.
- [33] Durganala, S. “Synthesis of Non-Halogenated Flame Retardants For Polyurethane Foams”, *Master of Science Thesis*, University of Dayton, The School of Engineering, Department of Chemical Engineering, August 2011.
- [34] *Development and Testing of Flame Retardant Additives and Polymers*, Final Report, Air Traffic Organization Operations Planning Office of Aviation Research and Development Washington, DC, April 2007.
- [35] Morgan, A.B. and Wilkie, (2014) C.A. *The Non-halogenated Flame Retardant Handbook*, Wiley. ISBN 9-781-118-93920-8.

- [36] Wilkie, C. A. and Morgan, A. B. (2009) *Fire Retardancy of Polymeric Materials*, CRC Press, Second Edition. ISBN 9-781-420-08400-9.
- [37] Afacan, G. C. “Thermal Characterization Of Composites Of Polyamide-6 and Polypropylene Involving Boron Compounds Via Direct Pyrolysis Mass Spectrometry”, *Thesis for Doctor Of Philosophy*, Middle East Technical University, Graduate School of Natural and Applied Sciences, Department of Polymer Science & Technology, September 2013.
- [38] Doğan, M., Erdoğan, S., Bayramlı, E. “Mechanical, thermal, and fire retardant properties of poly (ethylene terephthalate) fiber containing zinc phosphinate and organo-modified clay”, *Journal of Thermal Analysis and Calorimetry*, **2013**; 112, 871-876.
- [39] Morgan A.B., Wilke C.A., “Flame Retardant Polymer Nanocomposites”, John Wiley & Sons, New Jersey, 2007.
- [40] Alexandre M., Dubois P., “Polymer-Layered Silicate Nanocomposites: Preparation, Properties and uses of A New Class of Materials”, *Materials Science and Engineering*, **2000**; 28, 1-63.
- [41] Gilman J. W., “Flammability and Thermal Stability Studies of Polymer Layered Silicate (clay) nanocomposites”, *Applied Clay Science*, **1999**; 15, 31-49.
- [42] Leszczynska A., Njuguna J., Pielichowski K., Banerjee J.R., “Polymer/Montmorillonite Nanocomposites with Improved Thermal Properties. Part

II. Thermal Stability of Montmorillonite Nanocomposites Based on Different Polymeric Matrixes”, *Thermochimica Acta*, **2007**; 454, 1-22.

[43] Leszczynska A., Njuguna J., Pielichowski K., Banerjee J.R., “Polymer/Montmorillonite Nanocomposites with Improved Thermal Properties. Part I. Factors Influencing Thermal Stability and Mechanisms of Thermal Stability Improvement”, *Thermochimica Acta*, **2007**; 453, 75–96.

[44] Shanmuganathan K., Deodhar S., Dembsey N., Fan Q., Calvert P.D., Warner S.B. “Flame Retardancy and Char Microstructure of Nylon-6/Layered Silicate Nanocomposites”, *Journal of Applied Polymer Science*, **2007**; 104, 1540-1550.

[45] Lewin M., “Some Comments on the Modes of Action of Nanocomposites in the Flame Retardancy of Polymers”, *Fire Materials*, **2003**; 27, 1–7.

[46] Saharil, J.; S.M. Sapuan, S. M. Natural Fibre Reinforced Biodegradable Polymer Composites, *Reviews on Advanced Materials Science*, **2011**; 30, 166-174.

[47] Pilla, S. Handbook of Bioplastics and Biocomposites Engineering Applications. (2011) Wiley-Scrivener. ISBN 978-0-470-62607-8.

[48] Effects of montmorillonite (MMT) on morphological, tensile, physical barrier properties and biodegradability of polylactic acid/starch/ MMT nanocomposites, *Journal of Thermoplastic Composite Materials*, **2015**; 28, 496–509.

- [49] Rafailovich, M.; Abecassis, D. Blend of immiscible polymers. Google Patents, 2007.
- [50] J. W. Gilman, C. L. Jackson, A. B. Morgan, R. Harris Jr, E. Manias, E. P. Giannelis, M. Wuthenow, D. Hilton and S. H. Phillips, *Chemistry of Materials*, **2000**; 12, 1866–1873.
- [51] S. Bourbigot, D. L. Vanderhart, J. W. Gilman, S. Bellayer, H. Stretz and D. R. Paul, *Polymer*, **2004**; 45, 7627–7638.
- [52] X. Zheng and C. A. Wilkie, *Polymer Degradation and Stability*, **2003**; 82, 441–450.
- [53] Serge Bourbigot, Gaëlle Fontaine, Flame retardancy of polylactide: an overview, *Polymer Chemistry*, **2010**; 1, 1413-1422.
- [54] Zhan, J., Wang, L., Hong, N., Hu, W., Wang, J., Song, L., Hu, Y. Flame-retardant and Anti-dripping Properties of Intumescent Flame-retardant Polylactide with Different Synergists, *Polymer-Plastics Technology and Engineering*, **2014**; 53, 387-394.
- [55] Bellucci F., Camino G., Frache A., Sarra A., “Catalytic Charring–Volatilization Competition in Organoclay Nanocomposites”, *Polymer Degradation and Stability*, **2007**; 92, 425-436.
- [56] Jang B. N., Costache M., Wilkie C. A., “The Relationship between Thermal Degradation Behavior of Polymer and the Fire Retardancy of Polymer/Clay Nanocomposites”, *Polymer*, **2005**; 46, 10678-10687.

- [57] Tang Y., Hu Y., Li B., Liu L., Wang Z., Chen Z., Fan W., “Polypropylene/Montmorillonite Nanocomposites and Intumescent, Flame-Retardant Montmorillonite Synergism in Polypropylene Nanocomposites”, *Journal of Polymer Science: Part A: Polymer Chemistry*, **2004**; 42, 6163-6173.
- [58] Hu Y., Wang S., Ling Z., Zhuang Y., Chen Z., Fan W., “Preparation and Combustion Properties of Flame Retardant Nylon 6/Montmorillonite Nanocomposite”, *Macromolecular Materials Engineering*, **2003**; 288, 272-276.
- [59] Tang Y., Hu Y., Wang S., Gui Z., Chen Z., Fan W., “Intumescent Flame Retardant–Montmorillonite Synergism in Polypropylene-Layered Silicate Nanocomposites”, *Polymer International*, **2003**; 52, 1396–1400.
- [60] Krishnamachari, P., Zhang, J., Lou, J., Yan, J., Uitenham, L. “Biodegradable Poly(Lactic Acid)/Clay Nanocomposites by Melt Intercalation: A Study of Morphological, Thermal, and Mechanical Properties.” *International Journal of Polymer Analysis and Characterization*, **2009**; 14, 336–350.
- [61] Bourmaud, A., Me, P., Kaci, M., Zaidi, L., Grohens, Y., Technologie, D., & Mate, L. “Relationship Between Structure and Rheological, Mechanical and Thermal Properties of Polylactide / Cloisite 30B Nanocomposites.” *Journal of Applied Polymer Science*, **2010**; 116, 1357–1365.

- [62] Araújo, a., Botelho, G., Oliveira, M., Machado, A. V. “Influence of clay organic modifier on the thermal-stability of PLA based nanocomposites.” *Applied Clay Science*, **2014**; 88-89, 144–150.
- [63] Meng, Q., Heuzey, M.-C., Carreau, P. J. “Control of thermal degradation of polylactide/clay nanocomposites during melt processing by chain extension reaction” *Polymer Degradation and Stability*, **2012**; 97, 2010–2020.
- [64] Wootthikanokkhan J., Cheachun T., Sombatsompop N., Thumsorn S., Kaabbuathong N., Wongta N., Wong-On J., Na Ayutthaya S. I., Kositchaiyong A., “Crystallization and thermomechanical properties of PLA composites: Effects of additive types and heat treatment”, *Journal of Applied Polymer Science*, **2013**; 129, 215–223.
- [65] Corcione, C. E.; Frigione, M. “Characterization of nanocomposites by thermal analysis”, *Materials*, **2012**; 5, 2960-2980.
- [66] Tian, H., Tagaya, H. “Preparation, characterization and mechanical properties of the polylactide/montmo-rillonite composites”, *Journal of Material Science*, **2007**; 42, 3244–3250.
- [67] Kolodov V .I., Shuklin S. G., Kutzenov A. P., Marakova L. G., Bystrov S. G., Demicheva O. V., Rudakova T. A., *Journal of Applied Polymer Science*, **2002**; 85, 1477–1483.

- [68] Bourbigot S. Le Bras M., Leeuwendal R., Shen K. K., *Polymer Degradation and Stability*; **1999**, 64, 419–425.
- [69] Carpentier F., Bourbigot S., Lebras M., Delobel R., Foulon M., *Polymer Degradation and Stability*, **2000**; 69, 83–92.
- [70] Standard Test Method for Tensile Properties of Plastics, ASTM International, 100 Barr Harbor Drive, PO Box C700, West Conshohocken, PA 19428-2959, United States.
- [71] UL-94-Test for Flammability of Plastic Materials for Parts in Devices and Appliances, Northbrook, IL: Underwriters Laboratories Inc., 1997.
- [72] Lewitus, D., McCarthy, S., Ophir, A., Kenig, S. “The effect of nanoclays on the properties of PLLA-modified polymers Part: 1 Mechanical and thermal properties”, *Journal of Polymer and the Environment*, **2006**; 14, 171-177.
- [73] Suprakas, S. R., Kazunobu, Y., Okamoto, M., Fujimoto, Y., Ogami, A., Ueda, K. “New polylactide/layered silicate nanocomposites. 5. Designing of materials with desired properties”, *Polymer*, **2003**; 44, 6633-6646.
- [74] Day, M., Nawaby, A. V., Liao, X. “A DSC Study of the crystallization behaviour of polylactic acid and its nanocomposites”, *Journal of Thermal Analysis and Calorimetry*, **2006**; 86, 623-629.

- [75] Chow, W. S., Lok, S. K. “Thermal properties of poly(lactic acid)/organo-montmorillonite nanocomposites”, *Journal of Thermal Analysis and Calorimetry*, **2009**; 95, 627-632.
- [76] Fukushima, K., Tabuani, D., Camino, G. “Poly(lactic acid)/clay nanocomposites: Effect of nature and content of clay on morphology, thermal and thermo-mechanical properties”, *Material Science and Engineering*, **2012**; 32, 1790-1795.
- [77] Krikorian, V., Pochan, D. J. “Unusual crystallization behaviour of organoclay reinforced poly(L-lactic acid) nanocomposites”, *Macromolecules*, **2004**; 37, 6480-6491.
- [78] Wu, T. M.; Wu, C. Y. Biodegradable poly(lactic acid)/chitosan-modified montmorillonite nanocomposites: Preparation and characterization, *Polymer Degradation and Stability*, **2006**; 91 2198-2204.
- [79] Pluta, M., Jeszka, J. K., Boiteux, G. “Polylactide/montmorillonite nanocomposites: Structure, dielectric, viscoelastic and thermal properties”, *European Polymer Journal*, **2007**; 43, 2819–2835.
- [80] Kiliaris P., Papaspyrides C. D. “Polymer/Layered Silicate (Clay) Nanocomposites: An overview of flame Retardancy”, *Progress in Polymer Science*, **2010**; 35, 902- 958.

- [81] Kaya, H. Özdemir, E., Kaynak, C. Hacaloglu, J. “Effects of nanoparticles on thermal degradation of polylactide/aluminium diethylphosphinate composites.” *Journal of Analytical and Applied Pyrolysis*; **2016** in press.

